Supporting Information for: Organophosphate Ester (OPE) Transport, Fate and Emissions in Toronto, Canada, Estimated using an Updated Multimedia Urban Model

Timothy F. M. Rodgers[1], Jimmy W. Truong[1], Liisa M. Jantunen[2,3], Paul A. Helm[4,5], Miriam L. Diamond[3,1,5*]

Number of Pages: 36

Number of Tables: 20 (including a separate file with three Microsoft Excel sheets containing Tables S10-S12)

Number of Figures: 12

[1]Department of Chemical Engineering and Applied Chemistry, University of Toronto, Toronto, Canada M5S 3E5
[2]Centre for Atmospheric Research Experiments, Environment and Climate Change Canada, Egbert, Canada L0L 1N0
[3]Department of Earth Sciences, University of Toronto, Toronto, Canada M5S 3B1
[4]Environmental Monitoring and Reporting Branch, Ontario Ministry of Environment and Climate Change, Toronto, Canada M9P 3V6
[5]School of the Environment, University of Toronto, Toronto, Canada M5S 3B1

1 Background on Organophosphate Esters

TDCiPP is an additive flame retardant, commonly used in upholstered furniture and spray and rigid polyurethane foam insulation[1]. In 2017, Canada proposed restricting the usage of TDCiPP in new mattresses and upholstered furniture to concentrations of 1000 mg kg^{-1} as a risk management measure to limit human exposure to TDCiPP, which may have reproductive and developmental toxic effects[1]. Environment and Climate Change Canada has not recommended controls on TDCiPP based on the risk to ecosystem health [1].

TCEP is also used as an additive flame retardant, primarily in building insulation, upholstered furniture and textiles[2]. The European Union moved to limit the use of TCEP in toys in 2012 due to the possibility of exposure to children and the subsequent possible risk of reproductive impacts and cancer[3]. Canada designated TCEP as "toxic" under the Chemicals Management Plan (CMP) in 2013[4]. The risk management measure implemented was prohibiting the use of TCEP in new toys intended for children under the age of three in 2014[5].

TDCiPP is another additive flame retardant used in upholstered furniture, children's foam products such as car seats and nursing pillows. Stapleton et al.[6] commented that TDCIPP has been identified as a primary replacement for penta-BDEs used in these applications. Hoffman et al.[7] found that urinary concentrations of the TDCiPP metabolite bis(1,3- dichloro-2-propyl) phosphate (BDCPP) were significantly higher in children than in adults, and that urine levels of BDCPP have been increasing dramatically since the phase-out of penta-BDE FRs. TDCiPP is listed under California's Proposition 65 that calls for mandatory labelling of products in which it is used. Canada has not recommended controls on TDCiPP due to low human and ecosystem exposure at current rates of usage[1].

The non-chlorinated OPE EHDPP is used as an additive plasticizer and FR in floor coverings, foam seating and bedding products[8], and has been reported as an ingredient in protective coatings for ships[9]. EHDPP is approved for usage in food packaging, from which it has been detected in food products[10].

TBOEP is used as an additive plasticizer and FR. It is commonly used in floor polishes, plastics, furniture and wall paper[11–13]. TBOEP has been shown to have negative impacts on reproduction in zebrafish and to change gene expression in *Daphnia Magna*[14,15]. We note that measurements of TBOEP are highly uncertain compared to measurements of other OPEs[16].

TPhP is used as an additive plasticizer and FR in electronic display monitors[17], and as a plasticizer in hydraulic fluid and in products such as nail polish[18]. TPhP has been shown to be acutely toxic to fish, shrimp and *Daphnia* sp. and to cause adverse developmental impacts as well as damage to carbohydrate metabolism, lipid metabolism, and the DNA damage repair system in zebrafish[2,19,20]. Carignan et al.[21] documented a significant decline by 38% of *in-vitro* pregnancy success rates in couples recruited through a fertility clinic, between the lowest and the highest quartiles of TPhP exposure, measured through urinary concentrations of the metabolite diphenyl phosphate (DPHP).

2 Model Description

We calculated the fugacity capacity of the modelled compartments using poly parameter linear free energy relationships (ppLFERS), which use the solvation parameters of Abraham[22] to calculate partitioning between phases. Although Abraham originally utilized separate equations for water-condensed phase partitioning and air-condensed phase partitioning, Goss[23] demonstrated that both partitioning systems can be predicted using a single linear free energy relationship (Equation S1):

$$logK_{i,j/u} = s_{j/u}S_i + a_{j/u}A_i + b_{j/u}B_i + l_{j/u}L_i + v_{j/u}V_i + c \quad \text{(S1)}$$

Equation S1 represents the partitioning of chemical *i* between compartments *j* and *u*. Small letters represent the system being modelled (e.g., air-water) while capital letters represent the chemical-specific Abraham's solute parameters. *S* is the dipolarity/polarizability, *A* the hydrogen bonding acidity, *B* the

hydrogen bonding basicity, *L* the non-specific Van der Waals interactions (represented by the hexadecane/air partitioning coefficient), *V* the McGowan molar volume (representing the size of cavity formed by solvation), and *c* is a fitting constant. The original equations also included an *E* term, representing the molar refractivity.

We also calculated the enthalpy of solvation ($dU_{i,j/u}$), used to adjust partition coefficients between phases based on temperature using Abraham's solvation parameters[24] (Table S1). We used measured values of the enthalpy of solvation in lieu of ppLFER-estimated values where available or we calculated the enthalpy of solvation for a particular system using the specified ppLFER when the equations existed in the literature; otherwise, we used the enthalpy of the closest analogous system. We adjusted the organic carbon-water system for temperature using the octanol-water enthalpy of solvation ($dU_{O/W}$), and we adjusted the storage lipid and aerosol-air partitioning coefficients for temperature using the octanol-air enthalpy of solvation ($dU_{O/A}$).

Table S1: Equations for partition constants $K_{i,j/u}$, (above the line) and enthalpies of sorption $dU_{i,j/u}$ (below the line), for a compound *i* between compartments *j* and *u*, as defined in the table.

System	Equation	Reference
Aerosol-Air (Q/A)	$logK_{i,A/Q} = 1.38S_i + 3.21A_i + 0.42B_i + 0.63L_i + 0.98V_i - 7.42$	25
Organic Carbon-Water (OC/W)	$logK_{i,OC/W} = -0.98S_i - 0.42A_i - 3.34B_i + 0.54L_i + 1.2V_i + 0.02$	26
Storage Lipid-Water (SL/W)	$logK_{i,SL/W} = -1.62S_i - 1.93A_i - 4.15B_i + 0.58L_i + 1.99V_i + 0.55$	27
Organic Carbon-Air (OC/A)	$K_{i,OC/A} = K_{i,OC/W}/K_{i,A/W}$	
Storage Lipid-Air (SL/A)	$K_{i,SL/A} = K_{i,SL/W}/K_{i,A/W}$	
Storage Lipid-Water (SL/W)	$dU_{i,SL/W} = -49.29S_i - 16.36A_i + 70.39B_i + 10.51L_i - 66.19V_i$	27
Octanol-Water (O/W)	$dU_{i,O/W} = -5.31S_i + 20.1A_i - 34.27B_i + 8.26L_i - 18.88V_i - 1.75$	28
Octanol-Air (O/A)	$dU_{i,O/A} = -6.04S_i + 53.66A_i + 9.19B_i + 9.66L_i - 1.57V_i + 6.67$	24
Water-Air (W/A)	$dU_{i,W/A} = -0.73S_i + 33.56A_i + 43.46B_i + 1.4L_i + 17.31V_i + 8.41$	24

Compartment-specific Z values (Z_j for compartment *j*) were calculated (Table S2) as described by Diamond et al.[29] and Mackay[30] with the exception of Z_Q for atmospheric particles for which we added a water layer to account for the growth of the particle with relative humidity (RH), as recommended by Arp et al[31]. They

observed that this layer contained a significant portion of chemical mass at over 90% RH for polar molecules in an air-particle system. We interpolated the growth factor of the particle from the measured values for unwashed Berlin particles[31].

Table S2: Z_j-values (mol m^{-3} Pa^{-1}) of sub-compartments (above the line) and bulk compartments (below the line) *j* used in ppLFER-MUM. R is the ideal gas constant (8.314 J mol^{-1} K^{-1}), T the temperature in Kelvin, VF the volume fraction of a sub-compartment and ρ (kg m^{-3}) the density of a compartment or sub-compartment. Compartments subscripts are as defined in the table.

Compartment	Equation
Gas-phase Air (A)	$Z_A = 1/RT$
Aerosol (Q)	$Z_Q = Z_A * \rho_Q * K_{Q/A} * \left(1 - VF_{Water\ in\ Q}\right) + Z_W * VF_{Water\ in\ Q}$
Dissolved Water (W)	$Z_W = 1/H$
Water Suspended Solids (SS)	$Z_{SS} = Z_W * K_{OC/W} * VF_{OC,SS} * \rho_{SS}$
Soil Solids (SQ)	$Z_{SQ} = Z_A * K_{OC/A} * VF_{OC,soil} * \rho_{soil}$
Sediment Solids (SedS)	$Z_{SedS} = Z_W * K_{OC/W} * VF_{OC,Sed} * \rho_{sed}$
Vegetation Storage (V)	$Z_V = Z_A * K_{SL/A}$
Dissolved Film (F)	$Z_F = Z_A * K_{SL/A}$
Film Particles (QF)	$Z_{QF} = Z_A * \rho_Q * K_{Q/A}$
Bulk Air	$Z_{A,Bulk} = Z_A + Z_Q * VF_{Q,A}$
Bulk Water	$Z_{W,Bulk} = Z_W + Z_{SS} * VF_{SS}$
Bulk Soil	$Z_{S,Bulk} = Z_A * VF_{A,S} + Z_W * VF_{W,S} + Z_{SQ} * VF_{Q,S}$
Bulk Sediment	$Z_{Sed,Bulk} = Z_W * VF_{W,Sed} + Z_{SedS} * VF_{Q,Sed}$
Bulk Vegetation	$Z_{V,Bulk} = Z_A * VF_{A,V} + Z_W * VF_{W,A} + Z_V * VF_V$
Bulk Film	$Z_{F,Bulk} = Z_F * VF_{OC,F} + Z_{QF} * VF_{QF,F}$

A "D Value" (mol Pa^{-1} h^{-1}) quantifies transport between compartments in a fugacity model. Multiplying a D value by the fugacity of the phase it is leaving gives the rate of chemical mass transfer (mol h^{-1}). For transformation reactions, the "reactive D value (D_R)" has the same form when used with a first order transformation rate constant (h^{-1}) k_i.

We modified the calculation of wet deposition to ensure that wet gas-phase deposition only applied to the compound in the gas-phase, and wet particle deposition only applied to the compound in the particle-phase

(Table S3). This modification was done to ensure that rain dissolution of the gas did not strip OPEs from the particle phase. We did not apply the intermittent rainfall correction of Jolliet and Hauschild[32] as initial tests showed that the model performance with and without the intermittent rainfall correction was similar and the correction significantly increased the complexity of the model parameterization.

Li et al.[33] proposed that the atmospheric reactivity of TDCIPP is retarded by the presence of atmospheric water, while Liu et al.[34] proposed that partitioning to the particle-phase similarly retards the oxidation of atmospheric OPEs. For PAHs, reactions with ozone on particle surfaces have been shown to increase the rate of reaction, dominating gas-phase reactions with the hydroxyl radical[35,36]. To account for these heterogeneous loss processes in the atmosphere, Kwamena et al.[37] adapted MUM to account for a different (in their case higher) rate constant for the fraction of chemical bound to particles. We adopted a lower transformation rate constant for the fraction of the chemical in the particle phase, as indicated by experimental results for OPEs[34,38]. We did the same for the urban film, under the assumption that the particle-bound fraction in the film would be similarly shielded from transformation (Table S3). The value of the rate constants is clearly an area of significant uncertainty and we note that the reactivity of other species in surface films, such as nitrous acid, may increase or decrease the rate of reaction[39].

Table S3: Original and modified D-Values (mol h^{-1} Pa^{-1}) for transformation in the air and film compartments. Reaction (D_{Rj}), wet gaseous deposition (D_{rj}) and wet aerosol deposition (D_{qj}) from the lower air compartment to any compartment j, with compartment subscripts as described in Table S2. For the soil, we also modified the dry aerosol deposition (D_{dS}). A (m^2) represents the area of a compartment, U_r (m h^{-1}) the rain rate, $f_{aerosol}$ the fraction of a compound bound to the aerosol, Q the aerosol scavenging ratio, U_p (m h^{-1}) the dry deposition rate of aerosol, If_w the vegetation wet interception fraction and If_d the vegetation dry interception fraction.

Equation from Diamond et al. (2001)	Equation used in ppLFER-MUM
$D_{RA} = V_A * Z_A * k_A$	$D_{RA} = V_A * [(1 - VF_{Q,A}) * Z_A * k_A + (VF_{Q,A}) * Z_Q$
$D_{RF} = V_F * Z_F * k_F$	$D_{RF} = V_F * [(1 - VF_{Q,F}) * Z_F * k_F + (VF_{Q,F}) * Z_{QF}$
$D_{rW} = A_W * U_r * Z_W$	$D_{rW} = A_W * U_r * Z_W * (1 - f_{aerosol})$
$D_{qW} = A_W * U_r * Q * VF_Q * Z_Q$	$D_{qW} = A_W * U_r * Q * VF_Q * Z_Q * f_{aerosol}$
$D_{rS} = A_S * U_r * Z_W$	$D_{rS} = A_S * U_r * Z_W * (1 - f_{aerosol}) * (1 - If_w)$
$D_{qS} = A_S * U_r * Q * VF_Q * Z_Q$	$D_{qS} = A_S * U_r * Q * VF_Q * Z_Q * (1 - f_{aerosol}) * (1 - If_w)$
$D_{dS} = A_S * U_P * VF_Q * Z_Q$	$D_{dS} = A_S * U_P * VF_Q * Z_Q * (1 - If_d)$
$D_{rV} = A_V * U_r * Z_W * If_w$	$D_{rV} = A_V * U_r * Z_W * If_w * (1 - f_{aerosol})$
$D_{qV} = A_S * U_r * Q * VF_Q * Z_Q * If_w$	$D_{qV} = A_W * U_r * Q * VF_Q * Z_Q * If_w * f_{aerosol}$
$D_{rF} = A_F * U_r * Z_W$	$D_{rF} = A_F * U_r * Z_W * (1 - f_{aerosol})$
$D_{qF} = A_F * U_r * Q * VF_Q * Z_Q$	$D_{qF} = A_F * U_r * Q * VF_Q * Z_Q * f_{aerosol}$

2.1 Model Parameterizations and Application

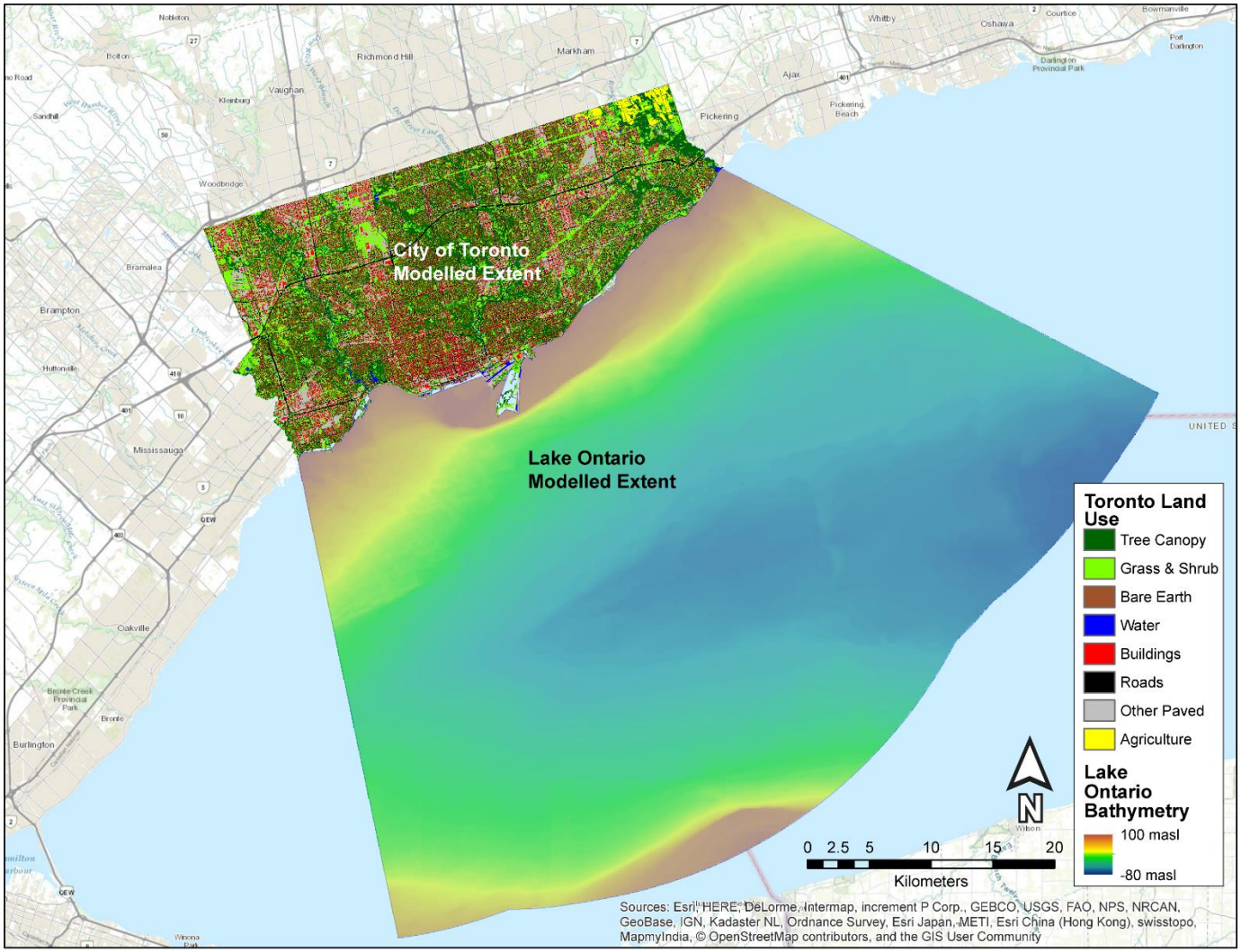

Figure S1: Map of the modeled areas of Toronto (the entire city) with bathymetry for the modelled section of Lake Ontario[40], showing the Toronto land-use data[41] used to calculate compartment areas. Basemap from ESRI[42].

131 The areas of the environmental compartments for Toronto were calculated based on Toronto land use data[41] and building dimensions[43] using

132 ArcMap version 10.5. The advective flow in the water compartment was the sum of the annual average flow from tributaries located within the

133 study area (Figure S1)[44]. All other values were taken from Csiszar et al.[45]. References in Table S5 are as noted.

134 Table S4: Compartment-specific physical parameters for the Toronto study area.

Parameter	Lower Air	Upper Air	Water	Soil	Sediment	Vegetation	Film	Lower Air (particles)	Upper Air (particles)
Area (m^2)	6.33E+08	6.33E+08	4.48E+06	3.37E+08	4.48E+06	4.07E+08	4.64E+08	-	-
Depth (m)	50	450	4.8	0.02	0.02	2.00E-03	1.00E-07	-	-
Density (kg m^{-3})	-	-	1000	2605	2400	850	1200	1500	1500
Fraction OC	-	-	-	0.06	0.04	0.05	0.05	0.2	0.2
Advective Flow (m^3 h^{-1})	3.60E+10	1.50E+11	5.60E+04		-	-	-	-	-

135

136 Table S5: Non-compartment-specific physical parameters for the Toronto study area.

Parameter	Value	Reference
Temperature (°C)	1.75E+01	Climate normal for Toronto, ON 1981-2010[46], May-October average
Rain Rate (m h^{-1})	1.01E-04	Climate normal for Toronto, ON 1981-2010[46], May-Oct average
Wind Speed (m s^{-1})	3.66E+00	Climate normal for Toronto Airport[46], ON 1981-2010, May-Oct average
Leaf Area Index (LAI)	1.22E+00	May - October average calculated from Gonsamo and Chen[47]
Relative Humidity (%)	6.96E+01	Climate normal for Toronto Airport, ON 1981-2010[46], May-Oct average
Upper/lower atmosphere transport rate u_a (m h^{-1})	8.18E+01	45
Air-side mass transport coefficient (MTC) over water k_{ma} (m h^{-1})	3.00E+00	48
Air-side MTC over water k_{mw} (m h^{-1})	3.00E-02	48
Scavenging ratio Q	2.00E+05	48
Dry Deposition velocity U_P (m h^{-1})	1.50E+00	As described below
Air-side MTC over soil k_{sa} (m h^{-1})	1.00E+00	48
β (kg m^{-2})	4.00E-01	29
Solid run-off rate from soil U_{sw} (m h^{-1})	1.01E-08	48
Water run-off rate from soil U_{ww} (m h^{-1})	5.06E-05	48
water-side MTC over sediment k_{xw} (m h^{-1})	1.00E-02	48
Sediment deposition rate U_{dx} (m h^{-1})	4.60E-08	48
Sediment resuspension rate U_{rx} (m h^{-1})	1.10E-08	48
Sediment burial rate U_{bx} (m h^{-1})	3.40E-08	48
Film wash-off rate constant W (h^{-1})	2.50E-01	29
Rainsplash rate constant R_s (h^{-1})	3.58E-07	29
Wet deposition interception loss fraction I_{lw}	1.90E-01	29
Canopy drip parameter λ	8.70E-04	29
MTC for wax erosion k_{we} (m h^{-1})	8.05E-08	29
1st-order litter fall rate constant Rlf (h^{-1})	2.31E-04	29
Upper air and stratosphere transfer rate U_{st} (m h^{-1})	1.00E-02	48
TSP (µg m^{-3})	3.75E+01	49
VFSusSed in water	1.25E-05	Using TSS = 30mg L^{-1}
VFAirinSoil	2.00E-01	50
VFWaterinSoil	3.00E-01	50
VFWaterinSed	8.00E-01	29
VFAirinVeg	1.80E-01	29
VFWaterinVeg	8.00E-01	29
VFLeafCuticle	2.00E-02	29
VFOCinFilm	3.00E-01	29
VFAerosolinFilm	7.00E-01	29

137

2.1.1 Dry Deposition Velocity

Csiszar et al.[45] used a chemical-specific dry particle deposition velocity, however, as these values were not available for the OPEs, we used a generic urban value of 1.5 cm per second[51–53]. The value chosen for OPEs neglected dry deposition velocities estimated over the ocean, which were an order of magnitude lower than the generic urban value used[54–56]. We rejected the over-ocean values for the model over Toronto as the deposition velocity is highly dependent on characteristics of the both atmospheric particles and the depositional surface. Specifically, dry depositional velocities are significantly greater over urban areas than over water[57,58]. We used the same value for all compounds.

2.1.2 Solute Descriptors

Solute descriptors (D_i) were selected using the UFZ-LSER database pre-selected values where available or estimated using the ACDLabs Absolv software[59], with the exception of the PCBs where the values of Van Noort et al.[60] were used for the S, A, B and V descriptors, and values from Abraham and Al-Hussaini[61] for L.

For analysis of trends in fate and physical chemical properties (Figure 2), we normalized the solute descriptors ($D_{N,i}$) for comparison with respect to the range of observed values for each solute descriptor (Equation S2, example calculations are shown for the L descriptor of EHDPP).

$$D_{N,i} = \frac{D_i}{D_{max} - D_{min}} \quad \text{(S2)}$$

$$L_{N,EHDPP} = \frac{12.83}{15.00 - 7.18} = 1.64$$

155 Table S6: Compound solute descriptors and references.

Compound	L	S	A	B	V	Reference
EHDPP	12.83	1.62	0.00	1.44	2.89	59
TBOEP	12.67	1.21	0.00	1.90	3.26	59
TCEP	7.18	2.09	0.03	0.98	1.76	62
TDCIPP	8.70	1.09	0.00	1.32	2.18	59
TDCIPP	9.93	2.10	0.03	1.24	5.55	62
TPhP	11.26	1.66	0.00	1.10	2.37	63
BDE-28	9.68	1.38	0.00	0.27	1.91	62
BDE-47	10.66	1.45	0.00	0.34	2.08	62
BDE-100	11.48	1.48	0.00	0.41	2.26	62
BDE-154	12.65	1.54	0.00	0.52	2.43	62
BDE-183	15.00	1.65	0.00	0.57	2.61	62
CB-28	7.90	1.35	0.00	0.10	1.60	60,61
CB-52	8.14	1.33	0.00	0.00	1.64	60,61
CB-101	9.30	1.47	0.00	0.00	1.76	60,61
CB-153	10.11	1.61	0.00	0.00	1.89	60,61
CB-180	10.42	1.75	0.00	0.00	2.01	60,61

156

157 ### 2.1.3 Physical-Chemical Properties

158 We calculated K_{AW} for the OPEs using Equations S3 and S4 as:

$$K_{AW} = H/RT \quad \text{(S3)}$$

$$H = P_L^o / C^S \quad \text{(S4)}$$

159 where H is the Henry's law constant, P_L^o the subcooled liquid vapor pressure, and C^S the water

160 solubility of the compound in question (Table S7).

161 Table S7: Vapor pressure and solubility values used in the calculation of K_{AW}.

Compound	Solubility (mol m^{-3})	Reference	LogP_L^o (Pa)	Reference
EHDPP	5.25E-03	64	8.91E-05	65
TBOEP	2.76E+00	66	6.81E-05	67
TCEP	2.46E+01	66	5.60E-02	67
TDCiPP	4.88E+00	68	3.48E-02	67
TDCiPP	1.62E-02	66	5.42E-04	67
TPhP	5.83E-03	64	3.57E-04	67

162

Table S8: Air-Water partition coefficients K_{AW}, enthalpies of sorption dU_j (kJ mol^{-1}), water and air diffusion coefficients β_j (m^2 h^{-1}), atmospheric OH radical reaction rate k_{OH} (mol OH h^{-1}), and water, soil and sediment reaction half-lives $T_{1/2,j}$ (h) used in this study.

Compound	$LogK_{AW}$[a,b]	dU_{AW}[b,c]	dU_{OW}[b,c]	dU_{OA}[b,d]	β_A[b,d]	B_W[b,d]	k_{OH}[b,e]	$T_{1/2,W}$[b,f]	$T_{1/2,S}$[b,g]	$T_{1/2,Sed}$[h]
EHDPP	-4.99	1.38E+05	-8.30E+00	1.36E+05	1.26E-06	1.34E-02	3.98E-11	7.80E+02	1.49E+03	3.24E+03
TBOEP	-7.82	1.64E+05	-3.02E+01	1.65E+05	1.15E-06	1.24E-02	1.29E-10	7.04E+02	8.16E+02	1.87E+03
TCEP	-5.86	9.10E+04	-1.98E+01	9.26E+04	1.66E-06	1.72E-02	2.20E-11	2.90E+03	1.46E+03	1.30E+04
TDCIPP	-5.36	1.15E+05	-2.21E+01	1.24E+05	1.45E-06	1.54E-02	4.48E-11	5.10E+03	1.46E+03	1.30E+04
TDCIPP	-4.69	1.72E+05	-7.76E+01	1.19E+05	1.31E-06	1.36E-02	1.81E-11	4.32E+03	1.46E+03	3.89E+04
TPhP	-4.43	1.12E+05	-3.43E-02	1.12E+05	1.44E-06	1.49E-02	1.08E-11	6.78E+02	1.00E+01	8.10E+03
BDE-28	-2.70	6.20E+04	-1.11E+01	6.20E+04	2.50E-06	3.90E-03	6.07E-13	2.50E+03	5.02E+03	1.30E+04
BDE-47	-3.12	6.60E+04	-3.06E+01	6.60E+04	2.40E-06	3.70E-03	4.31E-13	4.61E+03	9.24E+03	3.89E+04
BDE-100	-3.78	5.70E+04	-2.85E+01	5.70E+04	2.30E-06	3.60E-03	2.37E-13	8.50E+03	1.70E+04	3.89E+04
BDE-154	-3.68	7.67E+04	-2.15E+01	7.67E+04	2.20E-06	3.40E-03	1.00E-13	1.57E+04	3.14E+04	3.89E+04
BDE-183	-4.28	6.56E+04	-2.39E+01	6.56E+04	2.20E-06	3.30E-03	7.17E-14	2.11E+04	4.22E+04	3.89E+04
CB-28	-1.93	5.18E+04	-2.66E+04	5.18E+04	2.02E-06	0.015948	1.04E-12	5.50E+03	1.00E+04	1.70E+04
CB-52	-1.96	5.38E+04	-2.75E+04	5.38E+04	1.94E-06	0.015228	5.90E-13	1.00E+04	1.70E+04	5.50E+04
CB-101	-2.08	6.52E+04	-1.93E+04	6.52E+04	1.88E-06	0.014436	3.00E-13	3.10E+04	1.00E+05	5.50E+04
CB-153	-2.13	6.82E+04	-2.66E+04	6.82E+04	1.82E-06	0.013752	1.60E-13	5.50E+04	5.50E+05	1.70E+05
CB-180	-2.51	6.90E+04	-2.61E+04	6.90E+04	1.76E-06	0.013104	1.00E-13	5.50E+04	1.00E+06	1.70E+05

Notes: [a] K_{AW} was calculated as described above for OPEs [b] Obtained from Schenker et al.[69] for PCBs and PBDEs. [c] dU_{AW} and dU_{OW} for OPEs were calculated using the ppLFERs in Table S1. [c] dU_{OA} values for OPEs were measured by Okeme et al.[67], except for EHDPP which is estimated by the ppLFER in Table S1. [d] β_A and β_W for OPEs were calculated by using the EPA online "Estimated Diffusion Coefficients in Air and Water" tool[70], substituting N for P. [e] k_{OH} for OPEs was obtained from EpiSuite[71]. [f] $T_{1/2,W}$ values for OPEs are literature values reported by Zhang and Sühring et al.[72]. [g] $T_{1/2,S}$ values for OPEs are from CATALOGIC, as reported by Zhang and Sühring et al. [72]. [h] $T_{1/2,Sed}$ values are from EpiSuite v4.1[71] for all compounds.

2.1.4 Measured Air & Water Concentrations

Toronto OPE air concentrations were taken from Abdollahi et al.[73]. The concentrations for EHDPP were obtained from the authors who did not report them. Toronto air concentrations of PCBs and PBDEs were taken from Melymuk et al.[74]. Toronto OPE stream and rain water concentrations were taken from Truong[75]. The Toronto stream concentrations for PCBs and PBDEs were measured in 2008 upstream of the mouths of the rivers using automatic samplers[76]. We adjusted the water concentrations of CB-28, -101 and -180 to account for co-elutions with other PCB congeners, based on their distribution in Aroclor mixtures[77].

Table S9: Measured upwind air ($C_{A,U}$) Toronto air ($C_{A,T}$) and Toronto geometric mean water concentrations (C_W) in Toronto used for back-calculating and evaluating the emissions estimates, respectively.

Compound	$C_{A,U}$ (g m^{-3})	$C_{A,T}$ (g m^{-3})	C_W (g m^{-3})
EHDPP	6.9E-12	2.6E-10	1.8E-05
TBOEP	7.9E-11	6.9E-10*	7.3E-04
TCEP	5.0E-11	7.7E-10	2.0E-04
TDCiPP	7.9E-11	6.7E-10	9.7E-04
TDCiPP	7.9E-11	1.5E-10	1.1E-04
TPhP	5.9E-10	1.1E-09	2.0E-05
BDE-28	1.3E-13	3.2E-13	6.9E-09
BDE-47	6.0E-12	1.4E-11	3.2E-07
BDE-100	0.0	5.4E-16	6.8E-08
BDE-154	5.0E-13	6.8E-13	4.4E-08
BDE-183	7.4E-13	1.4E-12	2.7E-08
CB-28	1.5E-11	2.8E-11	6.6E-08
CB-52	1.7E-11	5.7E-11	7.4E-08
CB-101	1.3E-11	4.3E-11	7.6E-08
CB-153	9.9E-12	2.2E-11	8.3E-08
CB-180	1.5E-12	6.0E-12	5.5E-08

*High blank concentrations in TBOEP measurements led to many samples being below the method detection limit (MDL). This estimate is based on the observed concentrations, counting those below the MDL as half of the MDL.

2.2 Sensitivity and Uncertainty Analysis

The model uncertainty and sensitivity analyses were performed using a Monte Carlo Simulation (MCS) of 57,597 trials. MCS requires a probability distribution function for each variable input parameter. We used a triangular distribution with the most likely value as the preferred option, and the maximum and minimum values reported by Zhang and Sühring et al.[72] for K_{AW} and the water and soil transformation half lives. For the gas-phase air transformation rate constant we assumed a triangular distribution with the minimum equal to the particle transformation rate as defined previously. We did not vary the sediment half life as none of the OPEs had a significant mass fraction in the sediment compartment, and transformation was low for the PCBs and PBDEs.

We used the reported standard deviation for the measured Abraham`s solvation parameters L, S, and B. In most cases, a single value was reported and so as a conservative estimate we used the reported standard deviation for the entire system for each of the parameters. We used the root mean squared errors (RMSE) of 0.30 for B, 0.82 for S and 0.41 for L[59] reported by ACD Labs based on external validation for B and S and on internal validation for L for EHDPP, TBOEP and TCEP. We did not vary the A or the V solvation parameters, because A was zero or close to zero for all OPEs, and because the reported error of V was negligible at less than 0.6 % of the calculated value. We assumed a normal distribution for both the measured and the estimated solvation parameters.

Csiszar et al.[45] undertook a detailed sensitivity analysis for MUM of the wind speed between the upper and lower compartments (u_a) and the dry deposition rate (U_p). We assumed a triangular distribution using the ranges they defined as the upper and lower bounds and the base-case parameter values as the most likely values.

For the rank sensitivity analysis, a value of positive one indicates a perfectly monotonic relationship between the input value and the output, where an increase in the input value is correlated with an

increase in the output, while a value of negative one indicates a negative monotonic relationship. Spearman's correlation coefficient is considered appropriate for calculating the sensitivity of a monotonic model, such as ppLFER-MUM[78].

The model input assumptions and results of the Monte Carlo analysis are provided separately as Excel spreadsheets. Table S10 lists the model input assumptions; Table S11 and Figures S2 and S3 give the sensitivity results; and Table S12 gives the summary output statistics of the 57,597 trials reported here.

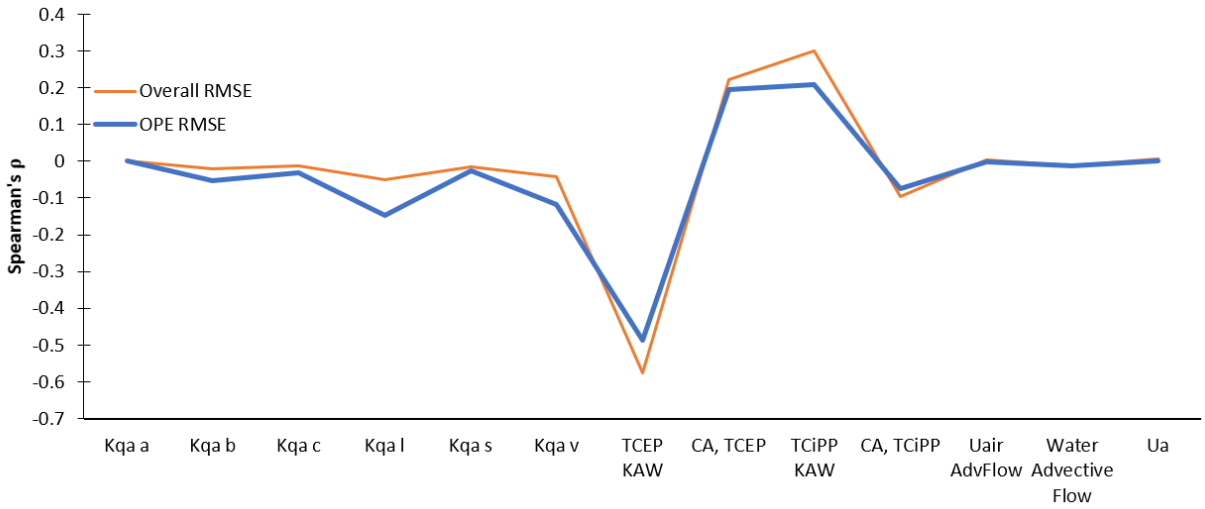

Figure S2: Sensitivity of the overall model RMSE to model input parameters, as measured by Spearman's correlation coefficient ρ. K_{AW} represents the air-water partition coefficient, target air concentration is the air concentration used in the back-calculation of emissions, the K_{QA} parameters are the gas-particle partition coefficient parameters in the ppLFER equation. All correlations shown had $p < 0.01$. Full sensitivity results are available in Table S11, including Excel charts showing all parameters.

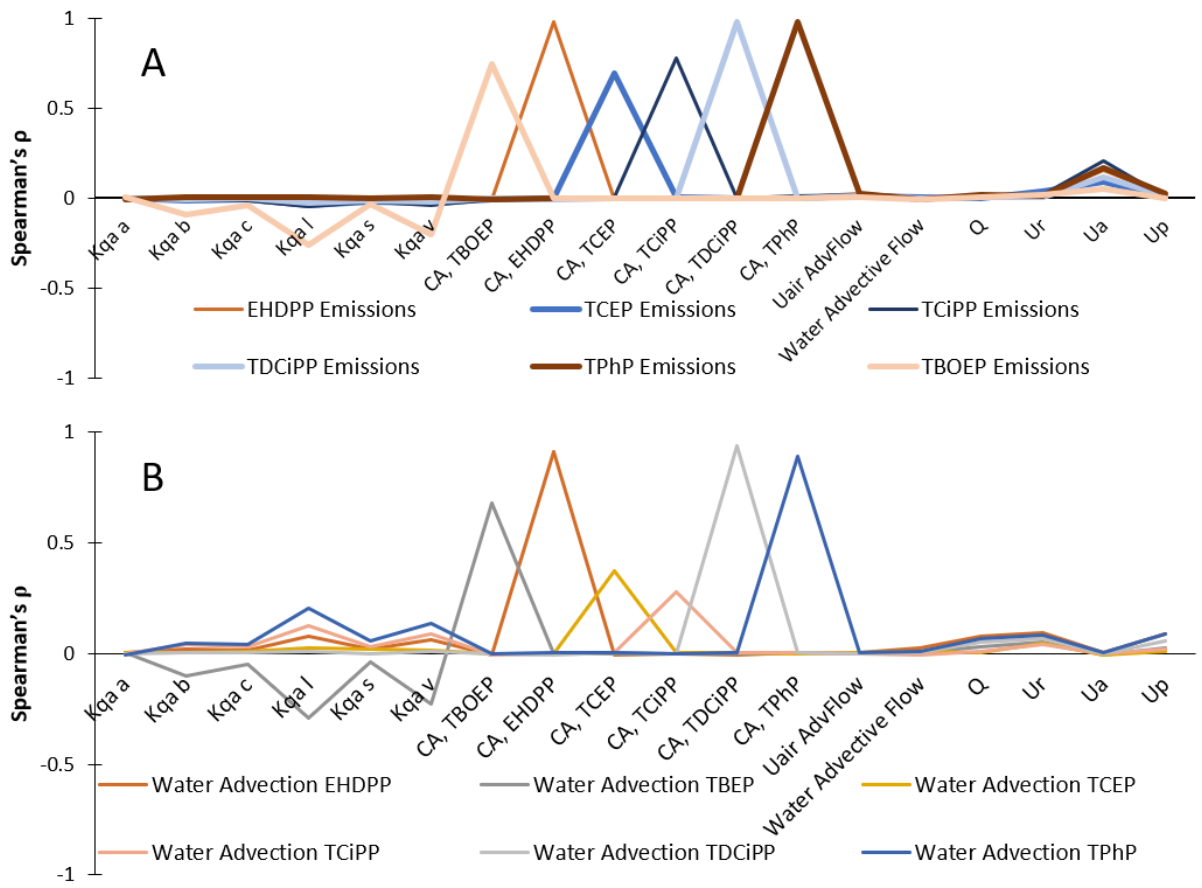

220

221 Figure S3: Sensitivity to model input parameters of: A) emissions, and B) stream loadings as water
222 advection (g/h) to Lake Ontario of TCEP, TDCiPP, TDCIPP, TPhP, EHDPP and TBOEP. Sensitivity was
223 expressed by Spearman's correlation coefficient ρ. CA,i represents the air concentration of compound i,
224 $K_{qa\,i}$ are the ppLFER system parameters for gas-particle partitioning, Q the scavenging ratio, U_r the rain
225 rate, U_a the upper and lower air transfer rate, and U_P the particle deposition rate. Full sensitivity results
226 are available in Table S11, including Excel charts showing all parameters.

227 ## 2.3 Loadings to Lake Ontario

228 Instantaneous loadings to nearshore Lake Ontario were calculated using Equation S5:

$$L = C\,x\,D \qquad \text{(S5)}$$

229 where L= loadings (kg day^{-1}), D = discharge (m^3 day^{-1}), and C = concentration (ng L^1) converted to kg m^{-3}.

230 Stream discharge for ΣOPEs ranged from 1.6 – 46 (m^3 s^{-1}) for Etobicoke Creek, 0.38 – 42 (m^3 s^{-1}) for the

231 Don River, and 0.39 – 51(m^3 s^{-1}) for Highland Creek. Loadings from WWTPs were calculated also

232 calculated using Equation S4, using the average daily discharge (D) from the wastewater treatment
233 plants. For the WWTPs, the annual average daily flow rates for 2014 and 2015 were as follows:
234 WWTP(A) 269-280 (ML day^{-1}), WWTP(B) 585-638 (ML day^{-1}), WWTP(C) 164-170 (ML day^{-1}). Each WWTP
235 had approximate catchment populations of 685,000, 1,524,000 and 509,000, respectively. Toronto has
236 one small WWTP with a flow of 0.02 ML day^{-1} which was not measured. To estimate these loadings we
237 used the average concentration from the other WWTPs to calculate loadings with Equation S4. Rain
238 loadings were calculated with a modified version of Equation S4, where the discharge was calculated as
239 the catchment area multiplied by the rain rate (m d^{-1}) observed during the sampling.

240 Instantaneous loadings to Toronto streams and stormwater from rainfall ranged from 0.68 – 14 kg day^{-1}.
241 This estimate assumed that rain fell evenly across the area of Toronto at the same concentration in one
242 day. These loadings represented just the pathway of emissions to air followed by runoff into tributaries
243 or WWTPs, without any additional capture of OPEs in the urban environment. Similar to wet weather
244 stream flows, rainfall is sporadic, and concentrations and volumes are likely to vary across the city, thus
245 the load estimates are likely to be biased high.

246 Estimated instantaneous loadings from the WWTPs ranged from 1.3–2.9 kg day^{-1} for Plant A to 2.0–7.8
247 kg day^{-1} for Plant B, and 0.21–1.9 kg day^{-1} for Plant C. Median WWTP(B) loadings were significantly
248 higher (3.7 kg day^{-1}) than the other plants (KWA-ANOVA, $p<0.05$), with the differences driven by mean
249 daily flows and the servicing of a larger portion of the population. The magnitude of the WWTP loadings
250 were similar to those for wet weather stream flows although unlike sporadic wet weather events,
251 WWTP the flows were more consistent day-to-day throughout the year. We extrapolated annual
252 average values from the ppLFER-MUM results for all Toronto streams, as explained in the main body of
253 this article. WWTP loadings were calculated from the measurements presented here.

254

Table S13: Daily flow, ΣOPEs concentration range and calculated instantaneous daily loading statistics for each watershed, WWTP and the rainfall. Low and high refer to discharge volumes in the hydrograph. "Etob" is short for Etobicoke.

	Daily Flow Range ($m^3 s^{-1}$)	**[OPE] Range ($\mu g L^{-1}$)**	**Minimum ($kg day^{-1}$)**	**Median ($kg day^{-1}$)**	**Maximum ($kg day^{-1}$)**	**Mean ($kg day^{-1}$)**	**Std. Error**
Etob Low (n=6)	0.37 - 1.7	1.2 - 3.1	0.048	0.092	0.31	0.14	0.043
Etob High (n=24)	0.99 - 42	1.3 - 8.1	0.42	2.8	17	4.1	0.85
Don Low (n=6)	1.6 - 3.2	1.3 – 4.8	0.21	0.44	1.5	0.63	0.20
Don High (n=20)	2.1 - 46	2 - 7.8	0.36	2.5	31	6.1	1.7
Highland Low (n=7)	0.39 - 0.59	0.47 - 2.3	0.018	0.074	0.099	0.067	0.010
Highland High (n=22)	0.48 - 52	0.79 - 5.3	0.071	1.4	13	2.8	0.80
WWTP(A) (n=8)	6.8 – 7.4	4.8 - 11	1.3	2.3	2.9	2.2	0.19
WWTP(B) (n=7)	1.9 – 2.0	3.4 - 12	2.0	3.7	7.8	4.5	0.79
WWTP(C) (n=10)	3.1 – 3.2	1.2 - 11	0.21	1.2	1.9	1.2	0.16
Rain (n=16)	7.3 - 250	0.39 - 4.7	0.68	3.5	14	5.3	4.0

Table S14: Instantaneous daily loadings (kg day^{-1}, geomean and standard deviation) of TCEP, TDCiPP, TDCiPP, TPhP, EHDPP and TBOEP for each watershed, WWTP and the rainfall calculated from measured concentrations. Low and high refer to discharge volumes in the hydrograph. "Etob" is short for Etobicoke.

	TCEP	**TDCiPP**	**TDCiPP**	**TPhP**	**EHDPP**	**TBOEP**
Don Low	0.036 (0.046)	0.18 (0.17)	0.021 (0.019)	0.0029 (0.0014)	0.0024 (0.00061)	0.16 (0.13)
Don High	0.28 (0.62)	0.99 (2.1)	0.11 (0.30)	0.015 (0.053)	0.015 (0.13)	0.94 (4.7)
Etob Low	0.0085 (0.009)	0.041 (0.052)	0.0038 (0.0027)	0.00082 (0.00058)	0.00079 (0.00055)	0.018 (0.023)
Etob High	0.18 (0.35)	0.97 (1.7)	0.095 (0.38)	0.016 (0.027)	0.011 (0.087)	0.47 (1.5)
Highland Low	0.0041 (0.0025)	0.020 (0.014)	0.0026 (0.00039)	0.00067 (0.00053)	0.00072 (0.0012)	0.016 (0.016)
Highland High	0.13 (0.15)	0.85 (1.3)	0.11 (0.19)	0.021 (0.038)	0.015 (0.035)	0.59 (2.3)
WWTP(A)	0.43 (0.23)	1.1 (0.77)	0.47 (0.33)	0.039 (0.15)	0.010 (0.0055)	1.1 (1.04)
WWTP(B)	0.081 (0.055)	0.21 (0.14)	0.12 (0.11)	0.0025 (0.00077)	0.0022 (0.000040)	0.47 (0.27)
WWTP(C)	0.20 (0.071)	0.46 (0.23)	0.31 (0.17)	0.012 (0.0082)	0.0036 (0.000078)	0.73 (0.40)
Rain	0.63 (1.1)	0.29 (0.61)	<MDL	0.042 (0.017)	<MDL	0.75 (2.0)

2.3.1 Loadings to Lake Ontario from Atmospheric Deposition

To estimate the loadings to Lake Ontario from atmospheric deposition attributable to Toronto, we ran a second version of ppLFER-MUM parameterized over Lake Ontario downwind of Toronto consisting of four compartments: lower air, upper air, water and sediment (Table S15). We defined the study area as a box 40 km out from the Toronto coast of Lake Ontario (Figure S1) and calculated the compartment dimensions using ESRI ArcMap version 10.5, with bathymetric data in Lake Ontario for the depth[40].

Table S15: Compartment-specific physical parameters for the Lake Ontario study area.

Parameter	Lower Air	Upper Air	Water	Sediment
Area (m^2)	2.5E+09	2.5E+09	2.5E+09	2.5E+09
Depth (m)	50	450	99	0.02
Density (kg m^{-3})	-	-	1000	2400
Fraction OC	-	-	-	0.04
Advective Flow (m^3 h^{-1})	2.8E+10	4.9E+11	4.1E+06	-

The advective flow for the water compartment was calculated by multiplying the mean current velocity in Lake Ontario of 1.0 m s^{-1} in the summer months[79] by the cross sectional area in the direction of flow.

We calculated the advective flow rate for the upper and lower air compartments by multiplying the average wind speed of the compartment by the cross-sectional area of the compartment in the direction of flow. To determine the average wind speed in the lower atmosphere of 3.8 m s^{-1}, we used wind speed data at an elevation of 10m from Toronto's Billy Bishop Airport[80], located on the Toronto coastline, taking the average wind speed blowing from Toronto to Lake Ontario, from South-South-West to North-East. For the upper atmosphere we calculated the average wind speed as 7.3 m s^{-1}, extrapolated from the value at 10 m using the wind profile power law to 275 m (the mean elevation of the upper air compartment), assuming an exponent of 0.2 based on average stability and negligible roughness[81] over the surface of the lake. Preliminary testing of the model sensitivity to the exponent, over a realistic range of 0.1 – 0.4, showed that modelled deposition changed by ≤10% of total loadings for all compounds, indicating that the model was not very sensitive to this parameter.

To calculate the inflow (g h^{-1}) to the upper and lower air compartments from Toronto, we calculated the proportion of time that winds blew from Toronto to Lake Ontario (as defined above) as approximately 53%. We then multiplied this factor by the advective flow from the upper and lower atmosphere modelled with ppLFER-MUM over Toronto (Table S16). To determine the inflow to the water compartment we used the sum of the stream and the WWTP loadings.

Table S16: Mass loadings (g h^{-1}) to the lower air, upper air and water compartments from Toronto to Lake Ontario. The range in brackets represents the 95% confidence interval around the base case from the uncertainty analysis.

Compound	Inflow to Lower Air	Inflow to Upper Air	Inflow to Water
TCEP	15 (1.8 – 57)	14 (0.3 – 120)	65 (18 – 1,300)
TDCiPP	24 (3.5 – 33)	11 (2.2 – 87)	86 (43 – 260)
TDCiPP	5.6 (0.2 – 14)	3.1 (3.7 – 49)	41 (22 – 84)
TPhP	38 (2.6 – 77)	21 (0.2 – 23)	11 (1.4 – 42)
EHDPP	9.4 (0.6 – 18)	5.3 (0.8 – 32)	2.9 (0.7 – 10)
TBOEP	25 (0.2 – 81)	14 (0.4 – 5.1)	100 (44 – 2,800)

We set the dry particle deposition velocity to 0.15 m h^{-1}, in line with measurements showing the dry deposition velocity of OPEs over water[54–56]. All other parameters were identical to those used in ppLFER-MUM over Toronto.

Table S17: Total loadings (through direct atmospheric deposition, streams and WWTP discharge) to Lake Ontario from Toronto.

Compound	Loadings (kg yr^{-1})	Loadings (mg m^{-2} yr^{-1})	Loadings (mg ca^{-1} yr^{-1})*
TCEP	670 (170 – 12,000)	1.0 (0.3 – 19)	260 (66 – 4,700)
TDCiPP	860 (390 – 2,500)	1.4 (0.6 – 3.9)	330 (150 – 930)
TDCiPP	370 (190 – 790)	0.6 (0.3 – 1.2)	140 (74 – 300)
TPhP	180 (17 – 530)	0.3 (0.0 – 0.8)	67 (6.5 – 200)
EHDPP	47 (7.8 – 150)	0.1 (0.0 – 0.2)	18 (3.0 – 56)
TBOEP	960 (380 – 24,000)	1.5 (0.6 – 38)	370 (150 – 9,200)
Σ_6OPEs	3,100 (1,200 – 40,000)	4.9 (1.8 – 64)	1,200 (450 – 15,000)

*Based on a Toronto population of 2.6 million[82]

Table S18: Direct atmospheric depositional OPE loadings to Lake Ontario from Toronto.

Compound	Loadings (kg yr^{-1})	Loadings (mg m^{-2} yr^{-1})	Loadings (mg ca^{-1} yr^{-1})*
TCEP	110 (11 – 530)	0.2 (0.0 – 0.8)	42 (4.2 – 200)
TDCiPP	110 (16 – 210)	0.2 (0.0 – 0.3)	41 (6.2 – 81)
TDCiPP	12 (2.4 – 54)	0.0 (0.0 – 0.2)	4.7 (0.9 – 21)
TPhP	81 (4.8 – 150)	0.1 (0.0 – 0.2)	31 (3.5 – 8.2)
EHDPP	22 (1.6 – 58)	0.0 (0.0 – 0.1)	11 (10 – 17)
TBOEP	57 (0.6 – 160)	0.1 (0.0 – 0.3)	18 (1.8 – 59)
Σ_6OPEs	390 (40 – 1,200)	0.6 (0.1 – 1.9)	150 (14 – 450)

*Based on a Toronto population of 2.6 million[82]

Table S19: Loadings through streams to Lake Ontario from Toronto.

Compound	Loadings (kg yr^{-1})	Loadings (mg m^{-2} yr^{-1})	Loadings (mg ca^{-1} yr^{-1})*
TCEP	300 (1.7 – 11,000)	0.5 (0.0 - 18)	120 (0.7 – 4,300)
TDCiPP	100 (0.3 – 1,200)	0.2 (0.0 – 1.9)	37 (0.1 – 460)
TDCiPP	16 (0.8 – 95)	0.0 (0.0 – 0.2)	6.0 (0.3 – 36)
TPhP	74 (5.9 – 300)	0.1 (0.0 – 0.5)	28 (2.3 – 120)
EHDPP	19 (1.7 – 80)	0.0 (0.0 – 0.1)	7.4 (0.6 – 30)
TBOEP	41 (0.7 – 22,000)	0.1 (0.0– 35)	16 (0.3 – 8,500)
Σ_6OPEs	550 (11 – 35,000)	4.7 (2.1 – 63)	210 (4.2 – 13,000)

*Based on a Toronto population of 2.6 million[82]

Table S20: Loadings through WWTPs to Lake Ontario from Toronto.

Compound	Loadings (kg yr^{-1})	Loadings (mg m^{-2} yr^{-1})	Loadings (mg ca^{-1} yr^{-1})
TCEP	260 (160 – 450)	0.4 (0.3 - 0.7)	100 (61 – 170)
TDCiPP	660 (680 – 1,100)	1.0 (0.6 - 1.7)	250 (140 – 410)
TDCiPP	340 (190 – 640)	0.5 (0.3 – 1.0)	130 (73 – 240)
TPhP	20 (6.2 – 69)	0.0 (0.0 – 0.1)	7.5 (2.4 – 27)
EHDPP	6.0 (4.5 – 8.4)	0.0 (0.0 – 0.0)	2.3 (1.7 – 3.2)
TBOEP	860 (380 – 1,700)	1.4 (0.6 – 2.8)	330 (150 – 670)
Σ_6OPEs	2,100 (1,100 – 4,000)	3.4 (1.8 – 6.3)	820 (430 – 1,500)

*Based on a Toronto population of 2.6 million[82]

3 Model Evaluation

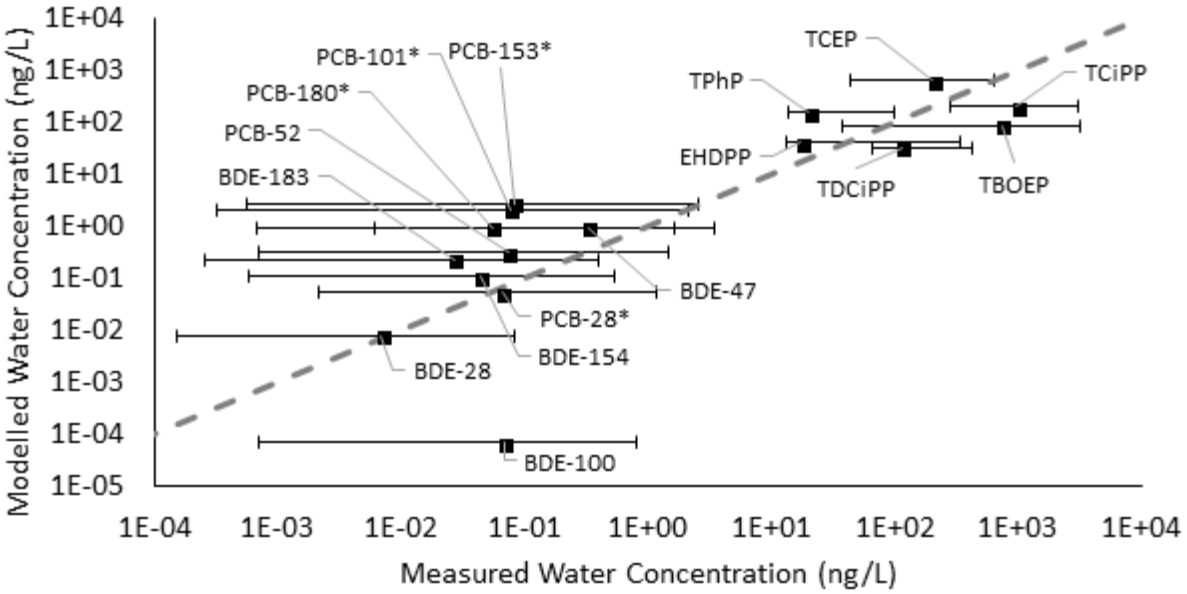

Figure S4: Measured vs modelled water concentration of OPEs, PBDEs and PCBs using ppLFER-MUM. Error bars represent the range for 95% of the measured concentrations while the squares represent the geometric mean values. The grey dashed line shows the 1:1 correlation between modelled and measured values. The measured PCB concentrations with an asterisk were adjusted to account for co-elution with other PCB congeners. Measured OPE concentrations from Truong[75], measured PCB and PBDE concentrations from Melymuk et al.[74].

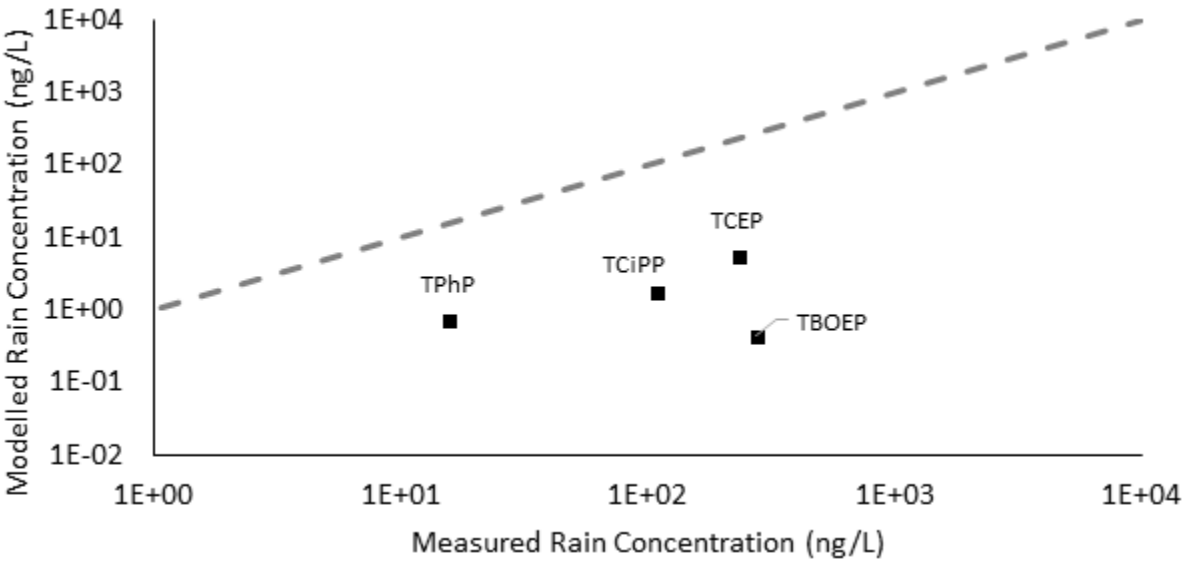

316

317 Figure S5: Measured vs modelled rain concentration of OPEs using ppLFER-MUM. The dashed line
318 represents 1:1 correspondence between measured and modeled concentrations.

319

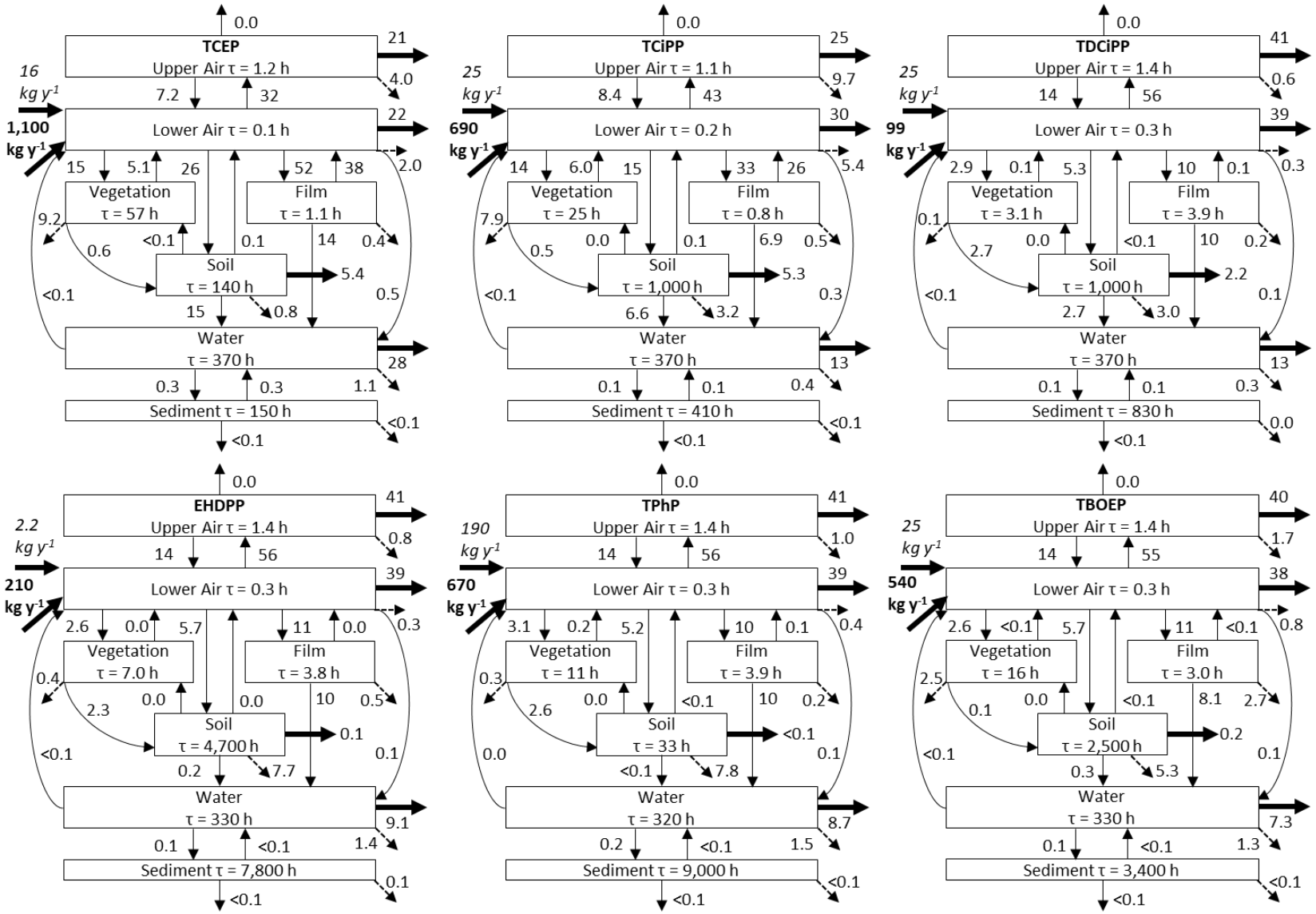

Figure S6: Schematic diagrams of the fate of six OPEs in seven compartments representing Toronto. Values in bold indicate the estimated aggregate emission rate to air (kg yr^{-1}), italics indicate the estimated upwind inflows (kg yr^{-1}), values beside arrows indicates rates of movement or transformation expressed as a percent of total atmospheric loadings (upwind inflows and emissions). Solid lines represent transfer between compartments, bold lines represent advection to or from the system, and dashed lines represent transformation. The residence time (τ) is given in hours for each compartment.

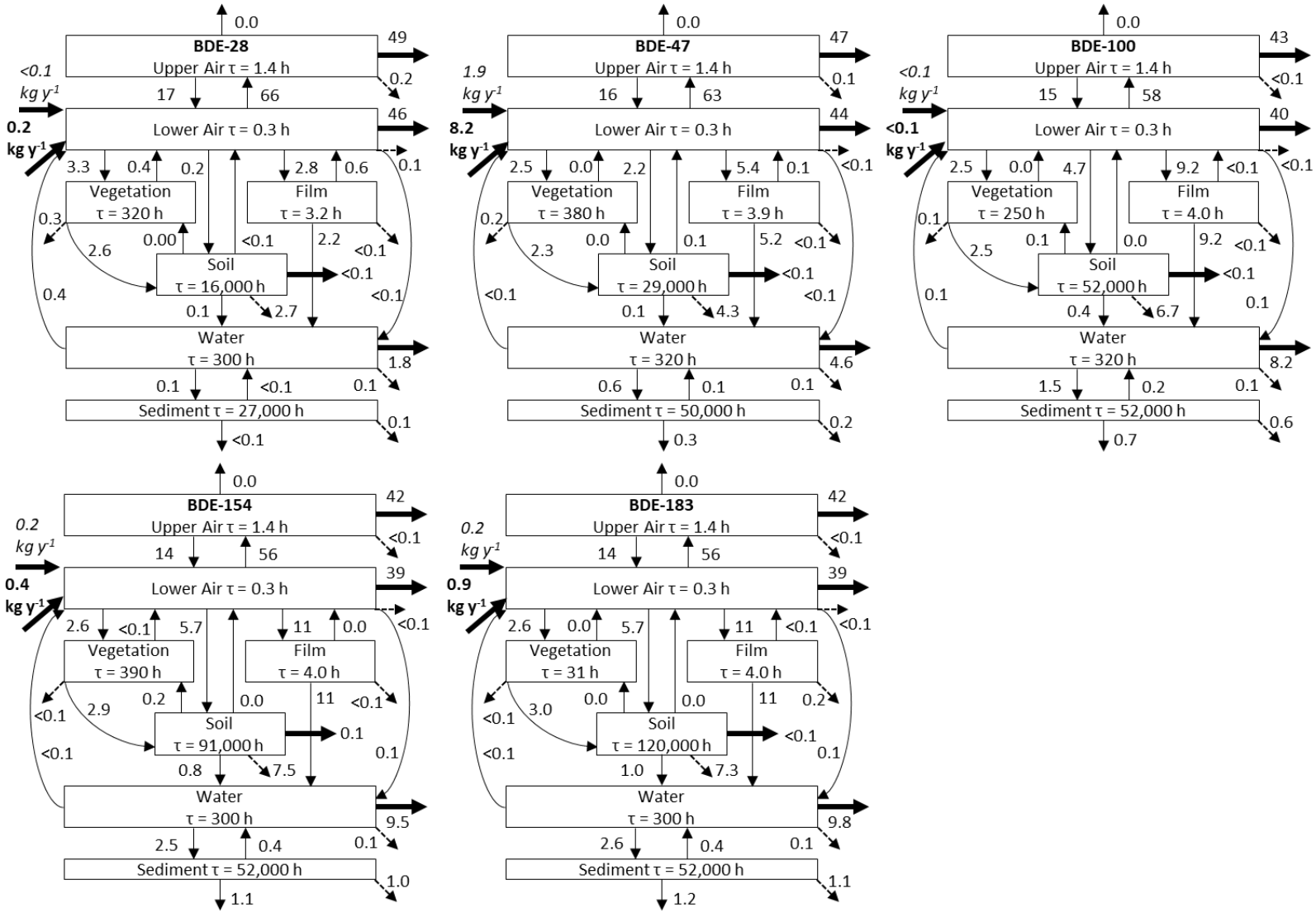

Figure S7: Schematic diagrams of the fate of five PBDEs in seven compartments representing Toronto. Values in bold indicate the estimated aggregate emission rate to air (kg yr^{-1}), italics indicate the estimated upwind inflows (kg yr^{-1}), values beside arrows indicates rates of movement or transformation expressed as a percent of total atmospheric loadings (upwind inflows and emissions) Solid lines represent transfer between compartments, bold lines represent advection to or from the system, and dashed lines represent transformation. The residence time (τ) is given in hours for each compartment.

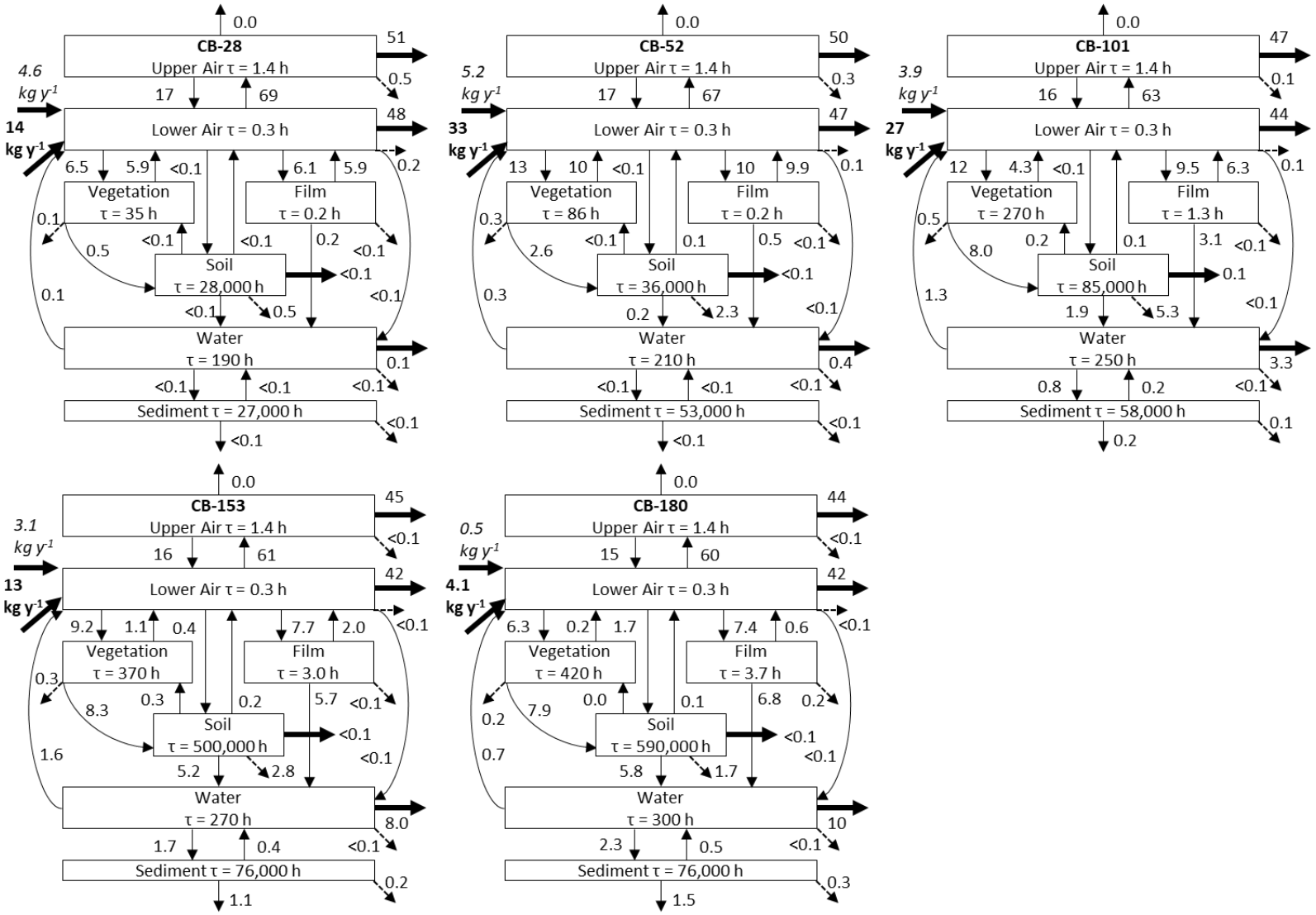

332

333 Figure S8: Schematic diagrams of the fate of five PCBs in seven compartments representing Toronto. Values in bold indicate the estimated
334 aggregate emission rate to air (kg yr^{-1}), italics indicate the estimated upwind inflows (kg yr^{-1}), values beside arrows indicates rates of movement
335 or transformation expressed as a percent of total atmospheric loadings (upwind inflows and emissions) Solid lines represent transfer between
336 compartments, bold lines represent advection to or from the system, and dashed lines represent transformation. The residence time (τ) is given
337 in hours for each compartment.

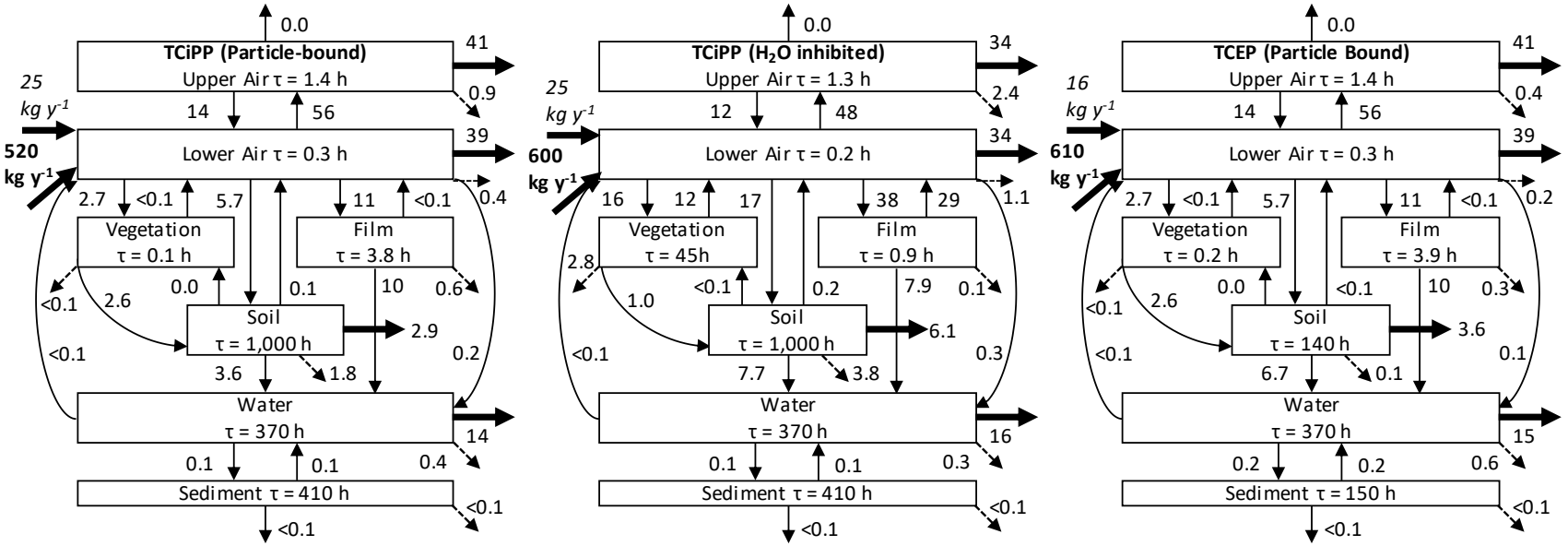

338

339 Figure S9: Results of the sensitivity analysis for TDCIPP and TCEP gas-particle partitioning and water-inhibited TDCIPP reaction constants. Values
340 in bold indicate the estimated aggregate emission rate to air (kg yr^{-1}), italics indicate the estimated upwind inflows (kg yr^{-1}), values beside arrows
341 indicates rates of movement or transformation expressed as a percent of total atmospheric loadings (upwind inflows and emissions) Solid lines
342 represent transfer between compartments, bold lines represent advection to or from the system, and dashed lines represent transformation.
343 The residence time (τ) is given in hours for each compartment.

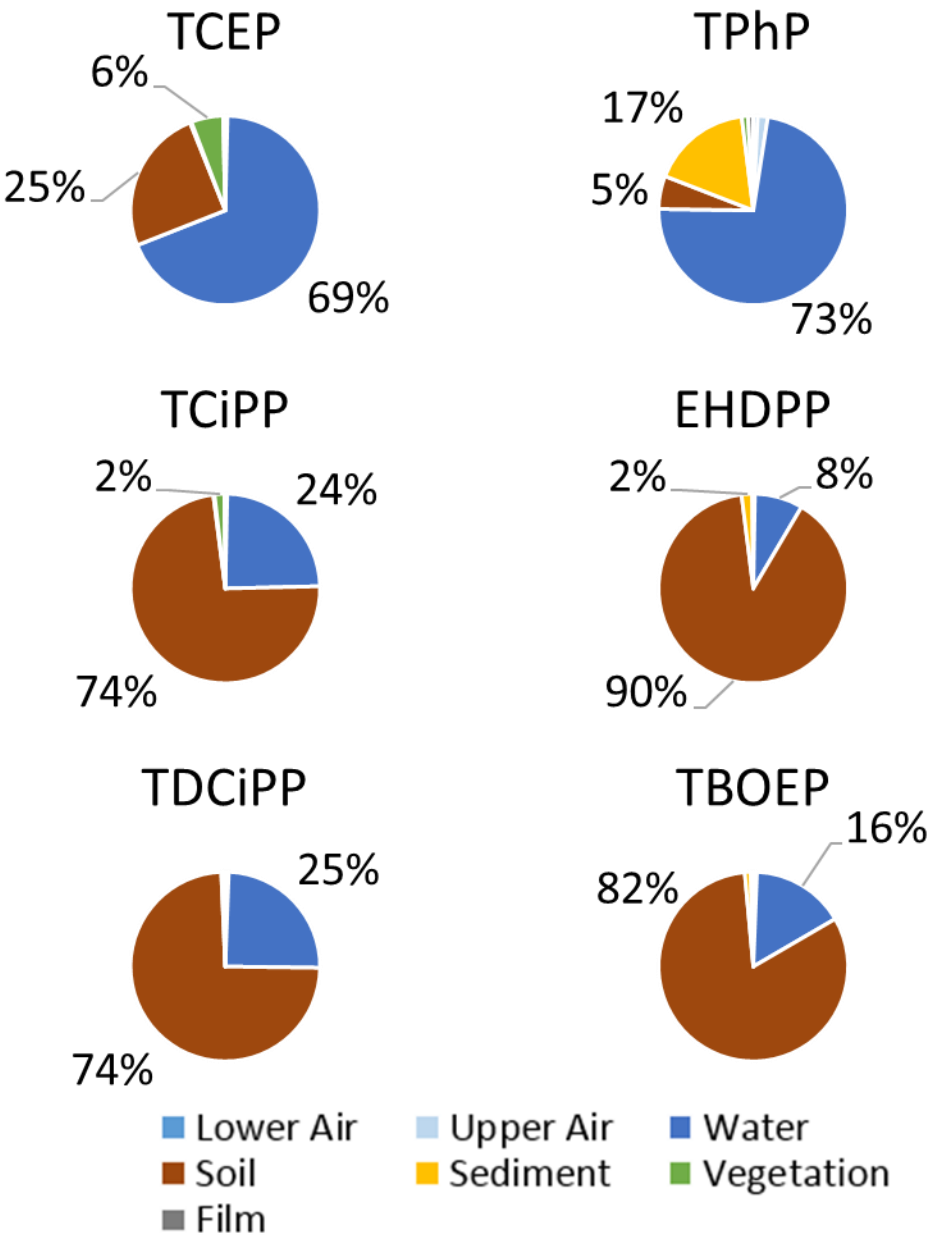

344

345 Figure S10: Mass distribution (% of total mass) of OPEs in modeled compartments of Toronto.

346

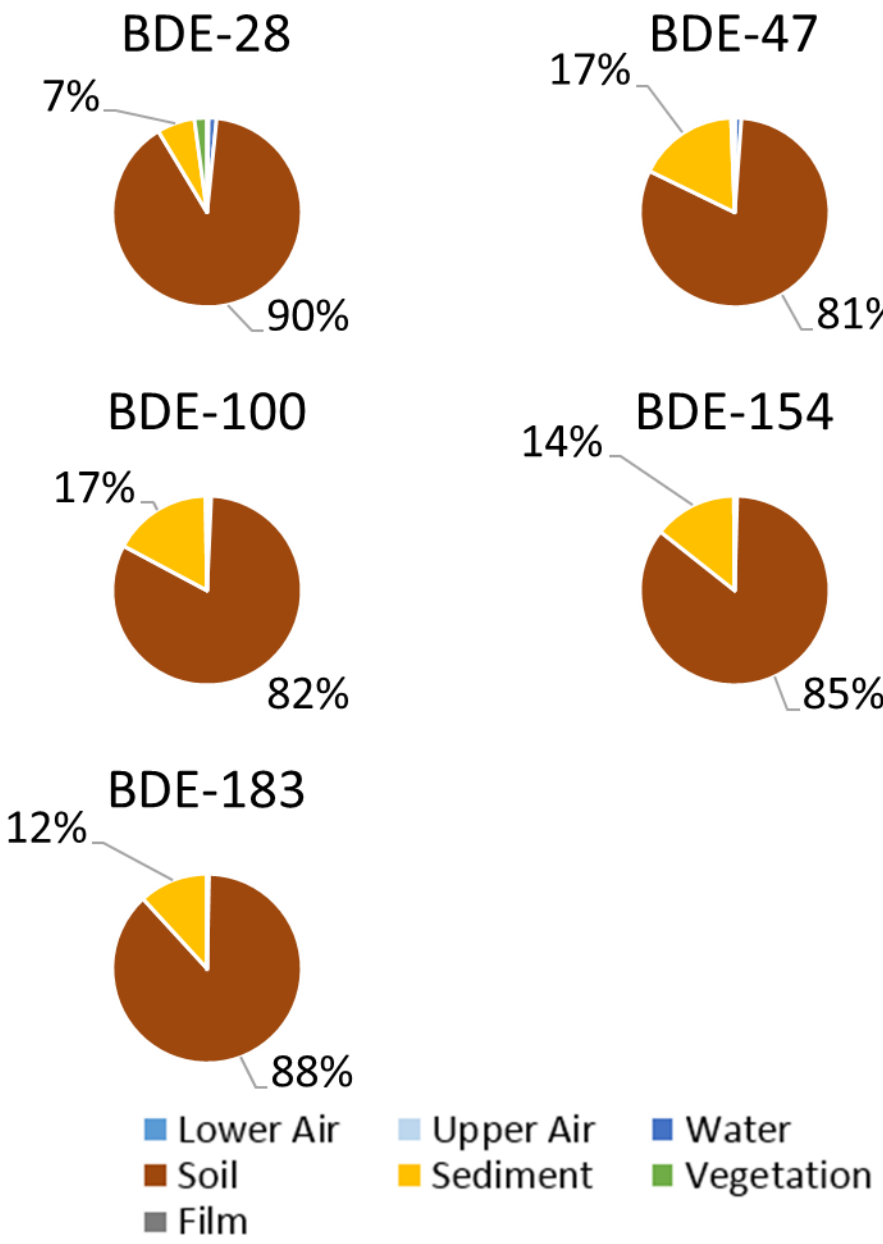

347

348 Figure S11: Mass distribution (% of total mass) of PBDEs in modeled compartments of Toronto.

349

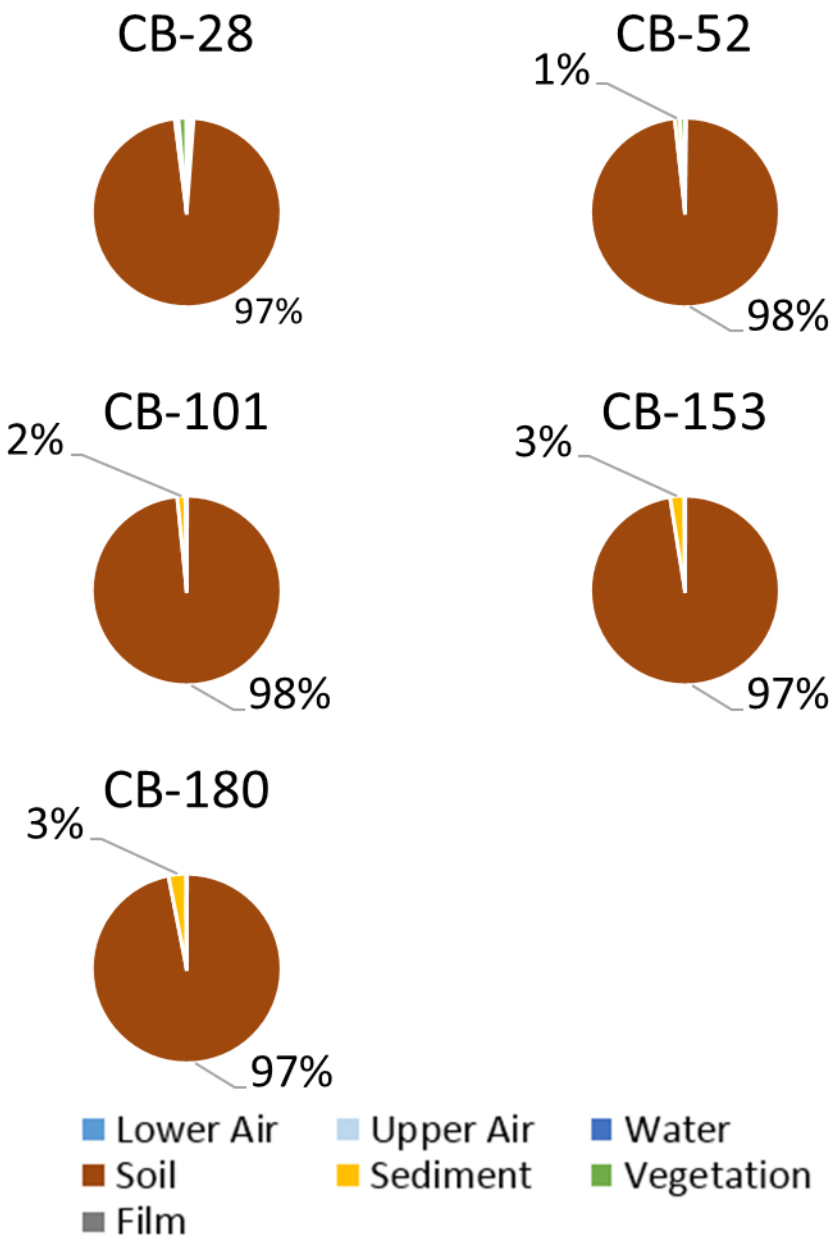

Figure S12: Mass distribution (% of total mass) of PCBs in modeled compartments of Toronto.

4 References

(1) Environment and Climate Change Canada. *Risk Management Scope for 2-Propanol, 1-Chloro-, Phosphate (3:1) (TCPP)*; 2016.

(2) van der Veen, I.; de Boer, J. Phosphorus Flame Retardants: Properties, Production, Environmental Occurrence, Toxicity and Analysis. *Chemosphere* **2012**, *88* (10), 1119–1153.

(3) Scientific Committee on Health and Environmental Risks (SCHER). *SCHER Opinion on Tris (2-Chloroethyl) Phosphate (TCEP) in Toys*; 2012.

(4) CEPA. *Order 2013-87-01-01 Amending the Domestic Substances List Persuant to Subsection 87(3) of the Act*; 2013.

(5) S.C. 2010, c. 21. *Regulations Amending Schedule 2 to the Canada Consumer Product Safety Act*; 2014.

(6) Stapleton, H. M.; Sharma, S.; Getzinger, G.; Ferguson, P. L.; Gabriel, M.; Webster, T. F.; Blum, A. Novel and High Volume Use Flame Retardants in US Couches Reflective of the 2005 PentaBDE Phase Out. *Environ. Sci. Technol.* **2012**, *46* (24), 13432–13439.

(7) Hoffman, K.; Butt, C. M.; Webster, T. F.; Preston, E. V.; Hammel, S. C.; Makey, C.; Lorenzo, A. M.; Cooper, E. M.; Carignan, C.; Meeker, J. D.; Hauser, R.; Soubry, A.; Murphy, S. K.; Price, T. M.; Hoyo, C.; Mendelsohn, E.; Congleton, J.; Daniels, J. L.; Stapleton, H. M. Temporal Trends in Exposure to Organophosphate Flame Retardants in the United States. Environ. Sci. Technol. Lett. 2017, 4 (3), 112–118.

(8) USEPA CDR. *Chemical Data Reporting for EHDPP*; 2017.

(9) Sundkvist, A. M.; Olofsson, U.; Haglund, P. Organophosphorus Flame Retardants and Plasticizers in Marine and Fresh Water Biota and in Human Milk. *J. Environ. Monit.* **2010**, *12* (4), 943.

(10) US Food and Drug Administration. US Food and Drug Administration - Total Diet Study Market Baskets 1991-3 through 2003-4: Summaries of Pesticide Analytical Results in Food from the Food and Drug Administration ' s Total Diet Study Program Summarized by Residue. **2006**, No. October 2003, i, 1-126.

(11) Marklund, A.; Andersson, B.; Haglund, P. Screening of Organophosphorus Compounds and Their Distribution in Various Indoor Environments. *Chemosphere* **2003**, *53* (9), 1137–1146.

(12) Yang, C.; Harris, S. A.; Jantunen, L. M.; Tsirlin, D.; Latifovic, L.; Fraser, B.; De La Campa, R.; You, H.; Kulka, R.; Diamond, M. L. Indoor Sources of and Human Exposure to Brominated Flame Retardants (BFRs), Organophosphate Esters (OPEs), and Phthalate Esters (PAEs). In *Proceedings of the 37th International Symposium on Halogenated Persistent Organic Pollutants*; 2017.

(13) Wang, Y.; Hou, M.; Zhang, Q.; Wu, X.; Zhao, H.; Xie, Q.; Chen, J. Organophosphorus Flame Retardants and Plasticizers in Building and Decoration Materials and Their Potential Burdens in Newly Decorated Houses in China. *Environ. Sci. Technol.* **2017**, *51* (19), 10991–10999.

(14) Giraudo, M.; Douville, M.; Houde, M. Chronic Toxicity Evaluation of the Flame Retardant Tris (2-

Butoxyethyl) Phosphate (TBOEP) Using Daphnia Magna Transcriptomic Response. *Chemosphere* **2015**, *132*, 159–165.

(15) Xu, Q.; Wu, D.; Dang, Y.; Yu, L.; Liu, C.; Wang, J. Reproduction Impairment and Endocrine Disruption in Adult Zebrafish (Danio Rerio) after Waterborne Exposure to TBOEP. *Aquat. Toxicol.* **2017**, *182*, 163–171.

(16) Stubbings, W. A.; Riddell, N.; Chittim, B.; Venier, M. Challenges in the Analyses of Organophosphate Esters. *Environ. Sci. Technol. Lett.* **2017**, *4* (7), 292–297.

(17) Kajiwara, N.; Noma, Y.; Takigami, H. Brominated and Organophosphate Flame Retardants in Selected Consumer Products on the Japanese Market in 2008. *J. Hazard. Mater.* **2011**, *192* (3), 1250–1259.

(18) Mendelsohn, E.; Hagopian, A.; Hoffman, K.; Butt, C. M.; Lorenzo, A.; Congleton, J.; Webster, T. F.; Stapleton, H. M. Nail Polish as a Source of Exposure to Triphenyl Phosphate. *Environ. Int.* **2016**, *86*, 45–51.

(19) Du, Z.; Zhang, Y.; Wang, G.; Peng, J.; Wang, Z.; Gao, S. TPhP Exposure Disturbs Carbohydrate Metabolism, Lipid Metabolism, and the DNA Damage Repair System in Zebrafish Liver. *Sci. Rep.* **2016**, *6* (October 2015), 21827.

(20) Behl, M.; Hsieh, J. H.; Shafer, T. J.; Mundy, W. R.; Rice, J. R.; Boyd, W. A.; Freedman, J. H.; Hunter, E. S.; Jarema, K. A.; Padilla, S.; Tice, R. R. Use of Alternative Assays to Identify and Prioritize Organophosphorus Flame Retardants for Potential Developmental and Neurotoxicity. *Neurotoxicol. Teratol.* **2015**, *52* (September), 181–193.

(21) Carignan, C. C.; Mínguez-Alarcón, L.; Butt, C. M.; Williams, P. L.; Meeker, J. D.; Stapleton, H. M.; Toth, T. L.; Ford, J. B.; Hauser, R. Urinary Concentrations of Organophosphate Flame Retardant Metabolites and Pregnancy Outcomes among Women Undergoing in Vitro Fertilization for the EARTH Study Team. *Environ. Health Perspect.* **2017**, *125* (8), 8.

(22) Abraham, M. H.; Andonian-Haftvan, J.; Whiting, G. S.; Leo, A.; Taft, R. S. Hydrogen Bonding. Part 34. The Factors That Influence the Solubility of Gases and Vapours in Water at 298 K, and a New Method for Its Determination. *J. Chem. Soc. Perkin Trans. 2* **1994**, No. 8, 1777.

(23) Goss, K.-U. Predicting the Equilibrium Partitioning of Organic Compounds Using Just One Linear Solvation Energy Relationship (LSER). *Fluid Phase Equilib.* **2005**, *233*, 19–22.

(24) Mintz, C.; Ladlie, T.; Burton, K.; Clark, M.; Acree, W. E.; Abraham, M. H. Enthalpy of Solvation Correlations for Gaseous Solutes Dissolved in Alcohol Solvents Based on the Abraham Model. *QSAR Comb. Sci.* **2008**, *27* (5), 627–635.

(25) Arp, H. P. H.; Schwarzenbach, R. P.; Goss, K.-U. Ambient Gas/Particle Partitioning. 2: The Influence of Particle Source and Temperature on Sorption to Dry Terrestrial Aerosols. *Environ. Sci. Technol.* **2008**, *42* (16), 5951–5957.

(26) Bronner, G.; Goss, K. U. Predicting Sorption of Pesticides and Other Multifunctional Organic Chemicals to Soil Organic Carbon. *Environ. Sci. Technol.* **2011**, *45* (4), 1313–1319.

(27) Geisler, A.; Endo, S.; Goss, K. U. Partitioning of Organic Chemicals to Storage Lipids: Elucidating

the Dependence on Fatty Acid Composition and Temperature. *Environ. Sci. Technol.* **2012**, *46* (17), 9519–9524.

(28) Ulrich, N.; Endo, S.; Brown, T. N.; Watanabe, N.; Bronner, G.; Abraham, M. H.; Goss, K.-U. UFZ-LSER Database http://www.ufz.de/lserd.

(29) Diamond, M. L.; Priemer, D. A.; Law, N. L. Developing a Multimedia Model of Chemical Dynamics in an Urban Area. *Chemosphere* **2001**, *44* (7), 1655–1667.

(30) Mackay, D. *Multimedia Environmental Models: The Fugacity Approach*, second.; Lewis Publishers: Boca Raton, 2001.

(31) Arp, H. P. H.; Schwarzenbach, R. P.; Goss, K. U. Ambient Gas/Particle Partitioning. 1. Sorption Mechanisms of Apolar, Polar, and Ionizable Organic Compounds. *Environ. Sci. Technol.* **2008**, *42* (15), 5541–5547.

(32) Jolliet, O.; Hauschild, M. Modeling the Influence of Intermittent Rain Events on Long-Term Fate and Transport of Organic Air Pollutants. *Environ. Sci. Technol.* **2005**, *39* (12), 4513–4522.

(33) Li, C.; Chen, J.; Xie, H.-B.; Zhao, Y.; Xia, D.; Xu, T.; Li, X.; Qiao, X. Effects of Atmospheric Water on ·OH-Initiated Oxidation of Organophosphate Flame Retardants: A DFT Investigation on TCPP. *Environ. Sci. Technol.* **2017**, *51* (9), 5043–5051.

(34) Liu, Y.; Liggio, J.; Harner, T.; Jantunen, L.; Shoeib, M.; Li, S. M. Heterogeneous OH Initiated Oxidation: A Possible Explanation for the Persistence of Organophosphate Flame Retardants in Air. *Environ. Sci. Technol.* **2014**, *48* (2), 1041–1048.

(35) Kwamena, N. O. A.; Thornton, J. A.; Abbatt, J. P. D. Kinetics of Surface-Bound Benzo[a]Pyrene and Ozone on Solid Organic and Salt Aerosols. *J. Phys. Chem. A* **2004**, *108* (52), 11626–11634.

(36) Kwamena, N. O. A.; Staikova, M. G.; Donaldson, D. J.; George, I. J.; Abbatt, J. P. D. Role of the Aerosol Substrate in the Heterogeneous Ozonation Reactions of Surface-Bound PAHs. *J. Phys. Chem. A* **2007**, *111* (43), 11050–11058.

(37) Kwamena, N. O. A.; Clarke, J. P.; Kahan, T. F.; Diamond, M. L.; Donaldson, D. J. Assessing the Importance of Heterogeneous Reactions of Polycyclic Aromatic Hydrocarbons in the Urban Atmosphere Using the Multimedia Urban Model. *Atmos. Environ.* **2007**, *41* (1), 37–50.

(38) Liu, Y.; Huang, L.; Li, S. M.; Harner, T.; Liggio, J. OH-Initiated Heterogeneous Oxidation of Tris-2-Butoxyethyl Phosphate: Implications for Its Fate in the Atmosphere. *Atmos. Chem. Phys.* **2014**, *14* (22), 12195–12207.

(39) Baergen, A. M.; Donaldson, D. J. Photochemical Renoxification of Nitric Acid on Real Urban Grime. *Environ. Sci. Technol.* **2013**, *47* (2), 815–820.

(40) National Geophysical Data Center (NGDC). Bathymetry of Lake Ontario. NOAA Satellites and Information 1999.

(41) Toronto Urban Forestry. Toronto Forest and Land Cover https://www.toronto.ca/city-government/data-research-maps/open-data/open-data-catalogue/#808bc73a-df10-284d-9df7-e60dc97b45ae.

(42) Esri. World Topographic Map. 2013.

(43) Toronto City Planning. 3D Massing https://www1.toronto.ca/wps/portal/contentonly?vgnextoid=d431d477f9a3a410VgnVCM10000071d60f89RCRD.

(44) Toronto and Region Conservation Authority (TRCA). Toronto and region watersheds: report card 2013 http://trca.on.ca/dotAsset/157180.pdf.

(45) Csiszar, S. A.; Daggupaty, S. M.; Verkoeyen, S.; Giang, A.; Diamond, M. L. SO-MUM: A Coupled Atmospheric Transport and Multimedia Model Used to Predict Intraurban-Scale PCB and PBDE Emissions and Fate. *Environ. Sci. Technol.* **2013**, *47* (1), 436–445.

(46) Environment and Climate Change Canada. Canadian climate normals 1981-2010 station data: Toronto, Ontario http://climate.weather.gc.ca/climate_normals/results_1981_2010_e.html?searchType=stnName&txtStationName=Toronto&searchMethod=contains&txtCentralLatMin=0&txtCentralLatSec=0&txtCentralLongMin=0&txtCentralLongSec=0&stnID=5051&dispBack=0.

(47) Gonsamo, A.; Chen, J. M. Improved LAI Algorithm Implementation to MODIS Data by Incorporating Background, Topography, and Foliage Clumping Information. *IEEE Trans. Geosci. Remote Sens.* **2014**, *52* (2), 1076–1088.

(48) Mackay, D.; Paterson, S.; Shiu, W. Y. Generic Models for Evaluating the Regional Fate of Chemicals. *Chemosphere* **1992**, *24* (6), 695–717.

(49) ECNAPS. *Environment Canada National Air Pollutant Suveillance Program*; 2017.

(50) Jones-Otazo, H. A.; Clarke, J. P.; Diamond, M. L.; Archbold, J. A.; Ferguson, G.; Harner, T.; Richardson, G. M.; Ryan, J. J.; Wilford, B. Is House Dust the Missing Exposure Pathway for PBDEs? An Analysis of the Urban Fate and Human Exposure to PBDEs. *Environ. Sci. Technol.* **2005**, *39* (14), 5121–5130.

(51) Tasdemir, Y.; Holsen, T. M. Measurement of Particle Phase Dry Deposition Fluxes of Polychlorinated Biphenyls (PCBs) with a Water Surface Sampler. *Atmos. Environ.* **2005**, *39* (10), 1845–1854.

(52) Raff, J. D.; Hites, R. A. Deposition versus Photochemical Removal of PBDEs from Lake Superior Air. *Environ. Sci. Technol.* **2007**, *41* (19), 6725–6731.

(53) Chen, L.; Peng, S.; Liu, J.; Hou, Q. Dry Deposition Velocity of Total Suspended Particles and Meteorological Influence in Four Locations in Guangzhou, China. *J. Environ. Sci.* **2012**, *24* (4), 632–639.

(54) Möller, A.; Xie, Z.; Caba, A.; Sturm, R.; Ebinghaus, R. Organophosphorus Flame Retardants and Plasticizers in the Atmosphere of the North Sea. *Environ. Pollut.* **2011**, *159* (12), 3660–3665.

(55) Castro-Jiménez, J.; González-Gaya, B.; Pizarro, M.; Casal, P.; Pizarro-Álvarez, C.; Dachs, J. Organophosphate Ester Flame Retardants and Plasticizers in the Global Oceanic Atmosphere. *Environ. Sci. Technol.* **2016**, *50* (23), 12831–12839.

(56) Lai, S.; Xie, Z.; Song, T.; Tang, J.; Zhang, Y.; Mi, W.; Peng, J.; Zhao, Y.; Zou, S.; Ebinghaus, R. Occurrence and Dry Deposition of Organophosphate Esters in Atmospheric Particles over the Northern South China Sea. *Chemosphere* **2015**, *127* (C), 195–200.

(57) Franz, T. P.; Eisenreich, S. J.; Holsen, T. M. Dry Deposition of Particulate Polychlorinated Biphenyls and Polycyclic Aromatic Hydrocarbons to Lake Michigan. *Environ. Sci. Technol.* **1998**, *32*, 3681–3688.

(58) González-Gaya, B.; Zúñiga-Rival, J.; Ojeda, M.-J.; Jiménez, B.; Dachs, J. Field Measurements of the Atmospheric Dry Deposition Fluxes and Velocities of Polycyclic Aromatic Hydrocarbons to the Global Oceans. *Environ. Sci. Technol.* **2014**, *48* (10), 5583–5592.

(59) ACD/Labs. Advanced Chemistry Development/I-Lab ABSOLV Predictor: **2017**.

(60) Van Noort, P. C. M.; Haftka, J. J. H.; Parsons, J. R. Updated Abraham Solvation Parameters for Polychlorinated Biphenyls. *Environ. Sci. Technol.* **2010**, *44* (18), 7037–7042.

(61) Abraham, M. H.; Al-Hussaini, A. J. M. Solvation Parameters for the 209 PCBs: Calculation of Physicochemical Properties. *J. Environ. Monit.* **2005**, *7* (4), 295–301.

(62) Stenzel, A.; Goss, K. U.; Endo, S. Determination of Polyparameter Linear Free Energy Relationship (Pp-LFER) Substance Descriptors for Established and Alternative Flame Retardants. *Environ. Sci. Technol.* **2013**, *47* (3), 1399–1406.

(63) Abraham, M. H.; Acree, W. E. Descriptors for the Prediction of Partition Coefficients and Solubilities of Organophosphorus Compounds. *Sep. Sci. Technol.* **2013**, *48* (6), 884–897.

(64) Saeger, V. W.; Hicks, O.; Kaley, R. G.; Michael, P. R.; Mieure, J. P.; Tucker, E. S. Environmental Fate of Selected Phosphate Esters. *Environ. Sci. Technol.* **1979**, *13* (7), 840–844.

(65) Brommer, S.; Jantunen, L. M.; Bidleman, T. F.; Harrad, S.; Diamond, M. L. Determination of Vapor Pressures for Organophosphate Esters. *J. Chem. Eng. Data* **2014**, *59* (5), 1441–1447.

(66) Mackay, D.; Shiu, W. Y.; Ma, K.; Lee, S. C. *Physical-Chemical Properties and Environmental Fate for Organic Chemicals*, Second Edi.; Taylor and Francis, 2006.

(67) Okeme, J. O.; Rodgers, T. M.; Parnis, J. M.; Diamond, M. L.; Jantunen, L. M. Vapour Pressures and Octanol-Air Partition Coefficients of Ultraviolet-Filters, Musks, Novel Brominated Flame Retardants (N-BFRs) and Organophosphate Esters (OPEs).

(68) WHO. Flame Retardants: Tris (Chloropropyl) Phosphate and Tris (2-Chloroethyl) Phosphate. *Environ. Heal. Criteria* **1998**, *209*, 129.

(69) Schenker, U.; Macleod, M.; Scheringer, M.; Hungerbühler, K. Improving Data Quality for Environmental Fate Models: A Least-Squares Adjustment Procedure for Harmonizing Physicochemical Properties of Organic Compounds. *Environ. Sci. Technol.* **2005**, *39* (21), 8434–8441.

(70) USEPA. EPA Estimated Diffusion Coefficients in Air and Water. 2017.

(71) US EPA. Estimation Programs Interface Suite™ for Microsoft® Windows, [v 4.11]. 2017.

(72) Zhang, X.; Sühring, R.; Serodio, D.; Bonnell, M.; Sundin, N.; Diamond, M. L. Novel Flame Retardants: Estimating the Physical–chemical Properties and Environmental Fate of 94 Halogenated and Organophosphate PBDE Replacements. *Chemosphere* **2016**, *144*, 2401–2407.

(73) Abdollahi, A.; Eng, A.; Jantunen, L. M.; Ahrens, L.; Shoeib, M.; Parnis, J. M.; Harner, T. Characterization of Polyurethane Foam (PUF) and Sorbent Impregnated PUF (SIP) Disk Passive Air Samplers for Measuring Organophosphate Flame Retardants. *Chemosphere* **2017**, *167*, 212–219.

(74) Melymuk, L.; Robson, M.; Helm, P. A.; Diamond, M. L. PCBs, PBDEs, and PAHs in Toronto Air: Spatial and Seasonal Trends and Implications for Contaminant Transport. *Sci. Total Environ.* **2012**, *429*, 272–280.

(75) Truong, J. W. Organophosphate Esters (OPEs) as Emerging Contaminants in the Environment: Indoor Sources and Transport to Receiving Waters, University of Toronto, 2016.

(76) Melymuk, L.; Robson, M.; Csiszar, S. A.; Helm, P. A.; Kaltenecker, G.; Backus, S.; Bradley, L.; Gilbert, B.; Blanchard, P.; Jantunen, L.; Diamond, M. L. From the City to the Lake: Loadings of PCBs, PBDEs, PAHs and PCMs from Toronto to Lake Ontario. Environ. Sci. Technol. 2014, 48 (7), 3732–3741.

(77) Frame, G. M.; Cochran, J. W.; Bøwadt, S. S. Complete PCB Congener Distributions for 17 Aroclor Mixtures Determined by 3 HRGC Systems Optimized for Comprehensive, Quantitative, Congener-Specific Analysis. *J. High Resolut. Chromatogr.* **1996**, *19* (12), 657–668.

(78) Gan, Y.; Duan, Q.; Gong, W.; Tong, C.; Sun, Y.; Chu, W.; Ye, A.; Miao, C.; Di, Z. A Comprehensive Evaluation of Various Sensitivity Analysis Methods: A Case Study with a Hydrological Model. *Environ. Model. Softw.* **2014**, *51*, 269–285.

(79) Beletsky, D.; Saylor, J. H.; Schwab, D. J. Mean Circulation in the Great Lakes. *J. Great Lakes Res.* **1999**, *25* (1), 78–93.

(80) Bayram, A.; Weller, L. *Porter Airlines Runway Extension Proposal Review Coastal Processes and Environments*; 2013.

(81) Touma, J. S. Dependence of the Wind Profile Power Law on Stability for Various Locations. *J. Air Pollut. Control Assoc.* **1977**, *27* (9), 863–866.

(82) Statistics Canada. Statistics Canada 2011 Census Toronto Population. **2011**.